iScience

CellPress
OPEN ACCESS

Article

Host macrocyclic acylcarnitines mediate symbiotic interactions between frogs and their skin microbiome

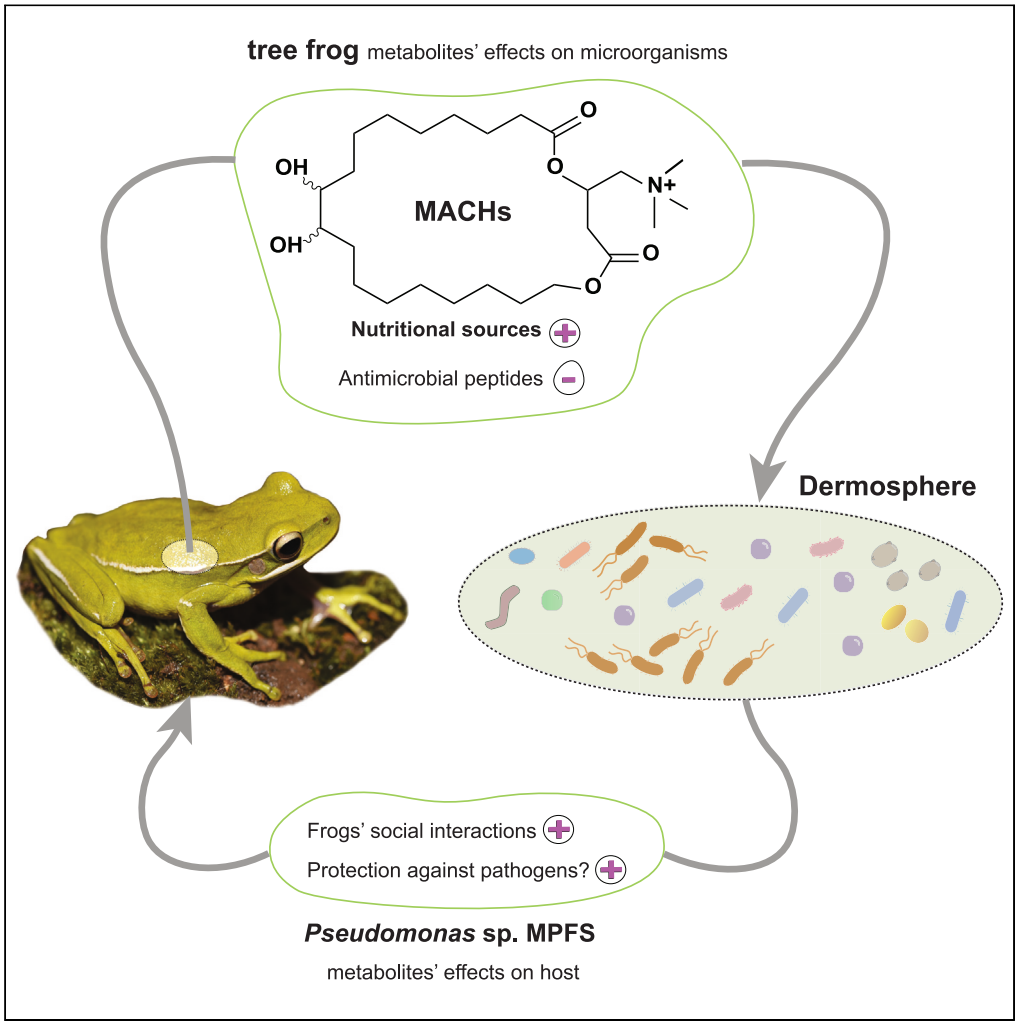

Andrés E. Brunetti, Mariana L. Lyra, Anelize Bauermeister, ..., Gabriela M. Cabrera, Jörg Overmann, Norberto P. Lopes

aebrunetti@conicet.gov.ar (A.E.B.)
joerg.overmann@dsmz.de (J.O.)
npelopes@fcfrp.usp.br (N.P.L.)

Highlights

Frogs' dermosphere is a rich source of metabolites mediating symbiotic interactions

The skin of tree frogs produces and secretes macrocyclic acylcarnitines

Pseudomonas is the most abundant genus of the frogs' skin bacterial community

Frogs' *Pseudomonas* symbionts can use acylcarnitines as the sole nutrient source

Brunetti et al., iScience 26, 108109
November 17, 2023 © 2023
https://doi.org/10.1016/j.isci.2023.108109

iScience

CellPress
OPEN ACCESS

Article

Host macrocyclic acylcarnitines mediate symbiotic interactions between frogs and their skin microbiome

Andrés E. Brunetti,[1,2,3,14,*] Mariana L. Lyra,[4] Anelize Bauermeister,[5] Boyke Bunk,[6] Christian Boedeker,[6] Mathias Müsken,[7] Fausto Carnevale Neto,[8] Jacqueline Nakau Mendonça,[2] Andrés Mauricio Caraballo-Rodríguez,[9] Weilan G.P. Melo,[10] Mônica T. Pupo,[10] Célio F.B. Haddad,[11] Gabriela M. Cabrera,[12,13] Jörg Overmann,[6,*] and Norberto P. Lopes[2,*]

SUMMARY

The host-microbiome associations occurring on the skin of vertebrates significantly influence hosts' health. However, the factors mediating their interactions remain largely unknown. Herein, we used integrated technical and ecological frameworks to investigate the skin metabolites sustaining a beneficial symbiosis between tree frogs and bacteria. We characterize macrocyclic acylcarnitines as the major metabolites secreted by the frogs' skin and trace their origin to an enzymatic unbalance of carnitine palmitoyltransferases. We found that these compounds colocalize with bacteria on the skin surface and are mostly represented by members of the *Pseudomonas* community. We showed that *Pseudomonas* sp. MPFS isolated from frogs' skin can exploit acylcarnitines as its sole carbon and nitrogen source, and this metabolic capability is widespread in *Pseudomonas*. We summarize frogs' multiple mechanisms to filter environmental bacteria and highlight that acylcarnitines likely evolved for another function but were co-opted to provide nutritional benefits to the symbionts.

INTRODUCTION

Several microorganisms have established symbiotic interactions with diverse plants and animal groups like cnidarians, mollusks, insects, and vertebrates, including humans.[1,2] In those cases where both partners benefit, the microorganisms can assist the host in nutrient assimilation,[3] pathogen defense,[4] and producing specialized metabolites used in social interactions.[5] In return, the host can offer suitable conditions for their microbial symbiont, such as a humid environment and nutrients,[1,6] and cooperate with them to inhibit microbial competitors.[4]

Among the organs exposed to the exterior world, the skin of vertebrates possesses specialized niches occupied by microorganisms interacting with each other and the host.[1,6] Given the plethora of associations and diversity of chemical components, this organ can be viewed as an ecosystem[7] exhibiting many parallelisms with the interface between plant roots and soil, the so-called rhizosphere.[8,9] Like the rhizosphere, the skin surface endures variable external mechanical and physicochemical conditions. Likewise, it is a rich chemical environment with various molecule classes like mucins, lipids, peptides, and specialized metabolites derived from both the host and the microbiota.[1,6] Also, similarly to plant metabolites in the rhizosphere, these substances may regulate the microbial community[10] by suppressing (e.g., through inhibition factors)[11,12] or stimulating (e.g., through nutrients) the growth of specific microbial consortia.[1] However, unlike the soil, skin components acting

[1]Instituto de Biología Subtropical (IBS, UNaM-CONICET), Posadas, Misiones N3300LQH, Argentina
[2]NPPNS, Department of Biomolecular Sciences, Faculty of Pharmaceutical Sciences of Ribeirão Preto, University of São Paulo, Ribeirão Preto, São Paulo 14040-903, Brazil
[3]Department of Insect Symbiosis, Max Planck Institute for Chemical Ecology, Hans-Knoell-Straße 8, 07745 Jena, Germany
[4]New York University Abu Dhabi, Saadiyat Island, Abu Dhabi 129188, United Arab Emirates
[5]Instituto de Ciências Biomédicas, Universidade de São Paulo, São Paulo 05508-000, Brazil
[6]Leibniz Institute DSMZ-German Collection of Microorganisms and Cell Cultures, 38124 Braunschweig, Niedersachsen, Germany
[7]Central Facility for Microscopy, Helmholtz Centre for Infection Research (HZI), 38124 Braunschweig, Niedersachsen, Germany
[8]Northwest Metabolomics Research Center, Department of Anesthesiology and Pain Medicine, University of Washington, 850 Republican Street, Seattle, WA 98109, USA
[9]Collaborative Mass Spectrometry Innovation Center, Skaggs School of Pharmacy and Pharmaceutical Sciences, University of California San Diego, La Jolla, CA, USA
[10]Faculdade de Ciências Farmacêuticas de Ribeirão Preto, Universidade de São Paulo, Ribeirão Preto, São Paulo 14040-903, Brazil
[11]Departamento de Biodiversidade e Centro de Aquicultura da UNESP (CAUNESP), Instituto de Biociências, UNESP-Universidade Estadual Paulista, Rio Claro, São Paulo 13506-900, Brazil
[12]Facultad de Ciencias Exactas y Naturales, Departamento de Química Orgánica, Universidad de Buenos Aires, Buenos Aires C1428EGA, Argentina
[13]Unidad de Microanálisis y Métodos Físicos aplicados a la Química Orgánica (UMYMFOR), Buenos Aires C1428EGA, Argentina
[14]Lead contact
*Correspondence: aebrunetti@conicet.gov.ar (A.E.B.), joerg.overmann@dsmz.de (J.O.), npelopes@fcfrp.usp.br (N.P.L.)
https://doi.org/10.1016/j.isci.2023.108109

as nutrient resources are limited and mostly unknown.[1,6] Therefore, it is a harsh environment where microorganisms capable of catabolizing host-derived metabolites have strong ecological advantages.

In contrast to the skin of other vertebrates, amphibian skin secretes several metabolites produced endogenously or obtained through diet, which include alkaloids, biogenic amines, odorous volatiles, peptides, and steroids, the reason why it was described as a mine of active compounds.[13,14] Still, although most of them have traditionally been studied as active agents against pathogens and predators, a new understanding of their biological functions and origin is currently emerging. For example, some of the compounds potentially mediating defensive functions[15] and sexual interactions[14] in the host are now known to be originated from symbiotic bacteria. In addition, these bacteria might produce metabolites like prodigiosin, sessilin, pyocyanin, and violacein that protect the host against the fungal pathogen *Batrachochytrium dendrobatidis*.[16,17] On the host side, the skin can actively select and establish specific bacterial assemblages from rare environmental strains.[18,19] This role was linked to amphibians' antimicrobial peptides and characterized as a filtering mechanism that structures the microbial community.[17,20] However, no study has assessed a more direct chemical benefit of the host to their symbionts, specifically, whether amphibians' skin metabolites can serve as a nutritional source for bacteria.

Here, we investigate the molecular determinants of the host that sustain an amphibian-bacteria symbiotic interaction. We used the tree frog *Boana prasina* and the bacterium *Pseudomonas* sp. MFPS[14] isolated from its skin as a frog-symbiont system. Through a combination of omics technologies, we demonstrated that macrocyclic acylcarnitines are major metabolites endogenously produced by the frog's skin glands, which are also present in the skin secretion of closely related species. Microscopy and mass spectrometry (MS) imaging revealed that these compounds are homogeneously distributed on the skin surface and colocalize with bacteria. Next, we examined the skin bacteria community structure of six frog species producing macrocyclic acylcarnitines and discovered that *Pseudomonas* is the most representative bacteria genus, suggesting that chemical and microbial profiles are closely linked. Through experiments with different carnitine derivatives, we show that *Pseudomonas* sp. MFPS catabolizes acylcarnitines and uses them for growth, while phylogenomic comparisons revealed that genes involved in such catabolism are widespread in *Pseudomonas*. Finally, using the rhizosphere as an ecological reference, we stress the significance of the dermosphere concept[21] as a fundamental means for surveying the skin environment subjected to the influence of metabolites secreted by both the host and the microbial symbionts.

RESULTS

Macrocyclic acylcarnitines are major components of frogs' skin secretion

We examined the chemical profile of the water-soluble components present in the skin glandular secretions of the tree frog *Boana prasina* and 33 other tree frog species from 11 genera in Argentina, Colombia, and Brazil (Figure 1A; Table S1). The sampling was designed to understand the evolutionary context of the compounds found in our model species *B. prasina*, emphasizing the closely related species within the *B. pulchella* group. Our analyses revealed that the skin secretion of *B. prasina* and other species of this group has a similar chemical profile. They share the major chromatographic peaks, and their respective MS fragmentation patterns conform to derivatives of the same molecular family (Figures 1B and 1C). To elucidate the chemical nature of these metabolites, we extracted and purified two of the main compounds secreted by *B. prasina* and analyzed them by high-performance liquid chromatography (HPLC)-quadrupole time of flight (QTOF)- tandem mass spectrometry (MS/MS), MS/MS-based fragmentation, gas chromatography-mass spectrometry (GC-MS), and 1D-2D nuclear magnetic resonance (NMR) spectroscopy (see STAR Methods for details). These compounds had the molecular formulas $C_{25}H_{48}NO_6$ and $C_{25}H_{46}NO_6$ and were designated MACH-1 and MACH-2, respectively (Figure 1D). Spectroscopic analysis revealed them as macrocyclic acylcarnitines containing a C18 fatty acid chain substituted by two hydroxyl groups and one unsaturated bond at the C-12′ position in MACH-2 (Figures S1–S12; Tables S2 and S3). GC-MS analysis of derivatized compounds indicated that the position of the hydroxyl groups is at C′9 and C′10 of the fatty acid chain (Figures 1D and S13). Based on the molecular networking and the MS/MS fragmentation pattern analysis of MACH-1 and MACH-2, other compounds within this acylcarnitines' molecular family were detected as part of the same homologous series (Figures 1C and S14–S18; Table S4). Although we observed compounds of this series in other species besides those within the *B. pulchella* group (Figure 1C), they only occurred as trace elements. The optical rotatory dispersion of MACH-1 was $[\alpha]_D^{25} = -16 \pm 4$.

Macrocyclic acylcarnitines are likely synthesized in frog's skin

Long-chain acylcarnitines are essential intermediates for the β-oxidation of fatty acids in the mitochondrial matrix and energy production.[23–25] For this reason, most studies have traditionally focused on organs and tissues with high energy demands, such as the skeletal muscle and the liver,[25] yet, none has examined their significance in the skin. Therefore, we studied the skin transcripts and the lipid profile of male and female specimens and conducted comprehensive research on lipid metabolism-related genes to understand better the accumulation of acylcarnitines and the generation of macrocycle derivatives in this organ. As a result, we found that all components of an enzyme system for the production of MACH-1 and MACH-2 are expressed in the skin of *Boana prasina* (Table 1; Data S1; Figure 2). Notably, it involves enzymes typically active in other tissues like the lung and liver meditating activation and ω-hydroxylation of long-chain fatty acids.

The biosynthesis would begin with the activation of the oleate and linoleate, occurring at high concentrations in the frogs' skin, by an acyl-coenzyme A (CoA) synthetase long chain (Tables 1 and S5; Figure 2). Afterward, these acyl-CoA thioesters would be conjugated with carnitine to form acylcarnitines by carnitine palmitoyltransferases (CPT1). Interestingly, we found that all three gene isoforms, CPT1A, CPT1B, and CPT1C, predominant in vertebrates' liver, muscle, and brain, respectively,[26,27] are expressed in the skin of *B. prasina,* albeit at different levels (Table 1; Data S1). The acylcarnitine esters would be initially accumulated in the skin gland because of the higher expression of CPT1 compared to CPT2 genes (4.1 and 4.7, in the female and male, respectively), which code for the enzyme responsible for the reconversion

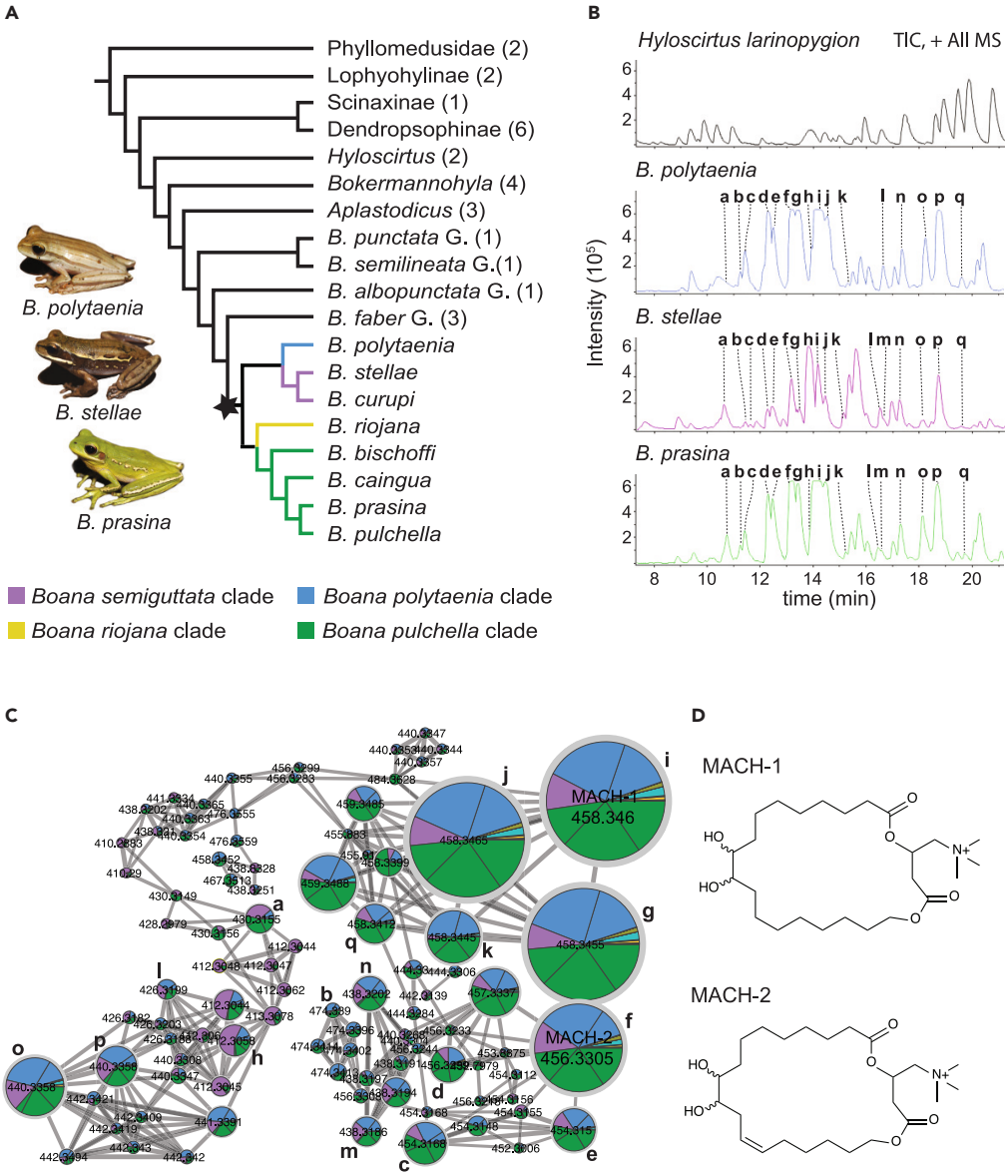

Figure 1. Macrocyclic acylcarnitines are major components of the skin secretion of tree frogs within the *Boana pulchella* group

(A) A condensed phylogenetic relationship based on the analysis from Faivovich et al.[22] of the South American tree frogs surveyed in this study. The star in the node indicates the root of the *Boana pulchella* group, whose representatives possess significant amounts of MACHs in their skin secretion. Blue, purple, yellow, and green branches correspond to the phylogenetic clades *B. riojana*, *B. polytaenia*, *B. semiguttata*, and *B. pulchella*, respectively. Images on the left depict representative specimens from the last three clades. Values in parentheses indicate the number of species examined.

(B) Total ion chromatograms in positive mode show the similar skin secretion profile of distinct clades within the *B. pulchella* group in contrast to the different profile of *Hyloscirtus larinopygion*.

(C) Based on LC-MS[2] (ESI+) spectral and retention time similarities, molecular networking revealed that the primary metabolites of these tree frogs are MACH analogs (a–q in *B*), occurring only in trace amounts in a few other species. Colors in pie charts depict the different phylogenetics clades shown in A.

(D) Structures of MACH-1 and MACH-2 were identified from the skin secretion of *Boana prasina* by a combination of NMR, MS, and derivatization, followed by GC-MS. The putative structure of other MACH analogs is depicted in Figure S14.

of acylcarnitines into the respective acyl-CoA esters and carnitine (Table 1; Data S1). Then, the synthesis would proceed through four reaction steps (Table 1; Data S1; Figure 2): (a) ω-hydroxylation mediated by cytochrome P450 family 4 subfamily B member 1, followed by (b) immediate cyclization, (c) epoxidation by a lipoxygenase such as arachidonate 5-lipoxygenase or another P450 monooxygenase, and (d) epoxide ring-opening and hydroxylation by an epoxide hydrolase such as the epoxide hydrolase 2. Given the limited information on macrocycles and diester of carnitines in vertebrates, we tentatively propose that the formation of the acylcarnitine macrocycle is mediated by the lactonizing activity of paraoxonase 2 or another unknown lipase.

Table 1. Sequence identity of proteins involved in fatty acid metabolism and their expression levels in the skin of *Boana prasina* in comparison to proteins reported from different tissues in humans and *Xenopus laevis*

	Humans		*Xenopus laevis*		*Boana prasina*	
Reaction/protein name	Uniprot Acc. nº	Identity %	Uniprot Acc. nº	Identity %	Female tpm	Male tpm
Fatty acid activation/						
acyl-CoA synthetase long-chain family member 1	P33121	76.2	Q7ZTJ3	85.5	0.6	2.5
acyl-CoA synthetase long-chain family member 3	O95573	74.4	A0A1L8G4N3	88.4	0.2	0.4
acyl-CoA synthetase long-chain family member 4	O60488	82.2	B3DLM0	89.5	0.2	0.6
Acylcarnitine formation/						
carnitine palmitoyltransferase 1A	P50416	78.6	A0A8J0V0P2	87.3	0.1	0.5
carnitine palmitoyltransferase 1B	Q92523	64.9	A0JMA3	82.4	2.9	5.6
carnitine palmitoyltransferase 1C	Q8TCG5	59.6	Q7ZWK5	88.1	0.3	0.7
Fatty acid and carnitine recovering						
carnitine palmitoyltransferase 2	P23786	72.6	Q7ZXE1	82.7	0.7	1.6
Omega-hydroxylation						
cytochrome P450 family 4 subfamily B member 1^{v1}	P13584	52.5	A0A8J0V6C5	68.8	0.8	1.2
cytochrome P450 family 4 subfamily B member 1^{v2}	P13584	52.9	A0A8J0V6C5	73.6	5.6	4.3
Acylcarnitine cyclization via *lactonization*						
paraoxonase 2	Q15165	56.9	Q6IRR7	65.2	1.0	0.9
Double bond oxygenation and epoxide opening						
arachidonate 5-lipoxygenase	P09917	78.3	A0A1L8FJT5	84.9	0.5	0.5
epoxide hydrolase 2	P34913	56.4	Q6DCH2	73.0	10.0	13.0

Acc. nº, accession number; v1, variant 1; v2, variant 2; tpm, transcripts per million.

Macrocyclic acylcarnitines colocalize with bacterial cells on the frog skin

Analysis of transverse sections and the surface of dorsal skin by matrix-assisted laser ionization (MALDI) imaging (using MS^1 and MS^2 experiments) and by transmission and scanning electron micrographs (Figures 3A, 3B, S19, and S20) showed that MACH-1 and MACH-2 are found within serous glands and are distributed homogeneously over the skin surface (Figure 3A). Because this distribution corresponds to the serous gland granules, we can assume that these compounds accumulate in the granules within the glands and are spread on the skin surface after the glands release their content (Figures 3B and S19). We detected no bacteria within serous glands (Figures S19 and S20). In contrast, we found mixed bacterial communities of cocci and bacilli with and without flagella on the skin surface, mainly concentrated in skin folds and gland pores, where they colocalize with MACH-1 and MACH-2 (Figure 3B).

Pseudomonas is prevalent in the bacterial skin community of its frog host

We systematically characterized the bacterial skin community of six species within the *B. pulchella* group from Brazil and Argentina using the V4 16S rRNA gene amplicon sequencing to explore a potential association between macrocyclic acylcarnitines and microorganisms. Alpha diversity was very similar between all populations except for two species from Argentina (*B. pulchella* [Fachinal, Misiones] and *B. stellae* [Cuñapiru, Misiones]), which showed higher and lower Faith phylogenetic diversity values, respectively (Figure S21). Eight genera at different abundance made up an average of 50% of the skin bacterial communities in all species of the *B. pulchella* group (Figure 3C). Notably, except for *B. polytaenia* from Serra da Bocaina (São Paulo, Brazil), *Pseudomonas* was the most representative genus in all frog populations, comprising 18%–50% of the abundance of the bacterial community. In contrast, the abundance of *Pseudomonas* in environmental samples was at a maximum of 8% (Figure 3C). Water samples and grass surfaces were dominated by an unidentified genus of the Comamonadacea family and *Methylbacterium* comprising 4%–20% and 35% of the bacterial community abundance, respectively.

Given the relevance of *Pseudomonas* sp. MPFS as a symbiont potentially mediating sexual interactions in *B. prasina*,[14] we examined the relative abundance of different *Pseudomonas* at the operational taxonomic unit (OTU) level (Figure 3D). Overall, 42 OTUs were identified as *Pseudomonas* in frog skin and environmental samples. Of them, 15 OTUs, including that representing the frog symbiont *Pseudomonas* sp. MPFS (OTU 14) and two OTUs (OTUs 13 and 20) with identical sequences to *Pseudomonas* strains previously isolated from *Boana prasina*,[14] were recovered in five or more frog populations from Argentina and Brazil with different relative abundances. However, none of them was found in all populations. Furthermore, despite one exception, these OTUs also occurred in environmental samples but at a much lower abundance. These findings suggest that environmental *Pseudomonas* can be found on the skin of tree frogs within the *B. pulchella* group, likely

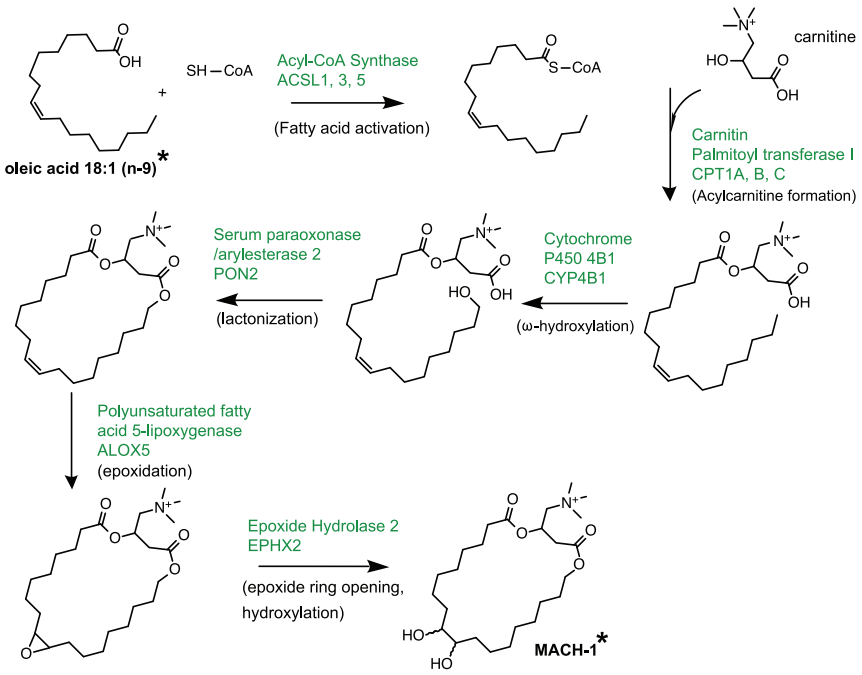

Figure 2. Putative biosynthetic pathway for skin macrocyclic acylcarnitines

Enzymes in green were identified and annotated from the skin transcriptome of *Boana prasina*. Compounds in bold and with an asterisk were identified in the skin lipid profile and secretion analyses. Following acylcarnitine accumulation, the pathway likely involves four reaction steps (depicted in brackets).

exploiting the host's conditions for establishing and growing. Thus, we explored how macrocyclic acylcarnitines could influence the growth of the frog symbiont *Pseudomonas* sp. MPFS isolated from the skin of *B. prasina*.

Pseudomonas symbionts can utilize acylcarnitine derivatives as nutrients

Given that *Pseudomonas aeruginosa* is an opportunistic pathogen capable of catabolizing acylcarnitines as sole carbon and nitrogen sources,[28–30] we test whether *Pseudomonas* sp. MPFS can utilize acylcarnitines from *B. prasina* as an energy source. We measured the growth of this bacterium in three minimal media containing L-carnitine and two commercially available L-acylcarnitines with ten- and 18-carbon chain lengths as sole carbon and nitrogen source, using *P. aeruginosa* PAO1 as a positive control. We found that the growth of both strains was higher on media supplemented with L-carnitine, sebacoyl-L-carnitine, and (*Z*,*Z*)-9-12-octadecanoyl-L-carnitine compared to the control without any supplement (Figure 4A). Compared to a control medium supplemented with glucose and NH_4 as carbon and nitrogen sources, the growth in the sebacoyl-L-carnitine medium was similar in *P. aeruginosa* PAO1 or slightly lower in *Pseudomonas* sp. MPFS (Figure 4B). However, both strains exhibited the maximum growth on (*Z*, *Z*)-9-12-octadecanoyl-L-carnitine. Notably, there was no stationary phase in the growth curve of *P. aeruginosa* PAO1, and a death phase immediately followed the log phase. Given the similarity between (*Z*,*Z*)-9-12-octadecanoyl-L-carnitine and MACH-2, in that the acyl chains of both compounds are derived from linoleate, we infer growth of *Pseudomonas* sp. MPFS is most likely similar on both compounds and the oleate derivative MACH-1.

Next, we screened the genome of *Pseudomonas* sp. MPFS for genes involved in the catabolism of carnitines using the known gene inventory of *P. aeruginosa* PAO1 as a guide.[29,31] This analysis confirmed that all genes and operons coding for enzymes involved in the metabolism and transcriptional regulation of carnitine to glycine and finally entering the central metabolism[28] are also present in the genome of *Pseudomonas* sp. MPFS (Figure 4B; Data S2). Furthermore, we assessed the frequency of these genes within the *Pseudomonas* genus in a dataset of orthologous proteins from 141 strains, including representatives of all known genus groups and subgroups within the *P. fluorescens* group. As shown in Figure 4B, the enzymes participating in the carnitine-catabolism pathways are widespread within *Pseudomonas*, except in the ancestral groups *P. pertucinogena*, *P. linyingensis*, and *P. stutzeri* and a few isolated strains. These findings suggest that several *Pseudomonas* species possess key ecological advantages to occupy the skin of frogs enriched in these compounds by utilizing L-acylcarnitines as a nutrient source for growth.

DISCUSSION

This study outlines the chemistry and molecular mechanisms underlying the interaction occurring on the skin of a diverse clade of tree frogs and their *Pseudomonas* symbionts. Based on our findings, we propose a chemical and ecological framework to investigate how symbiosis on

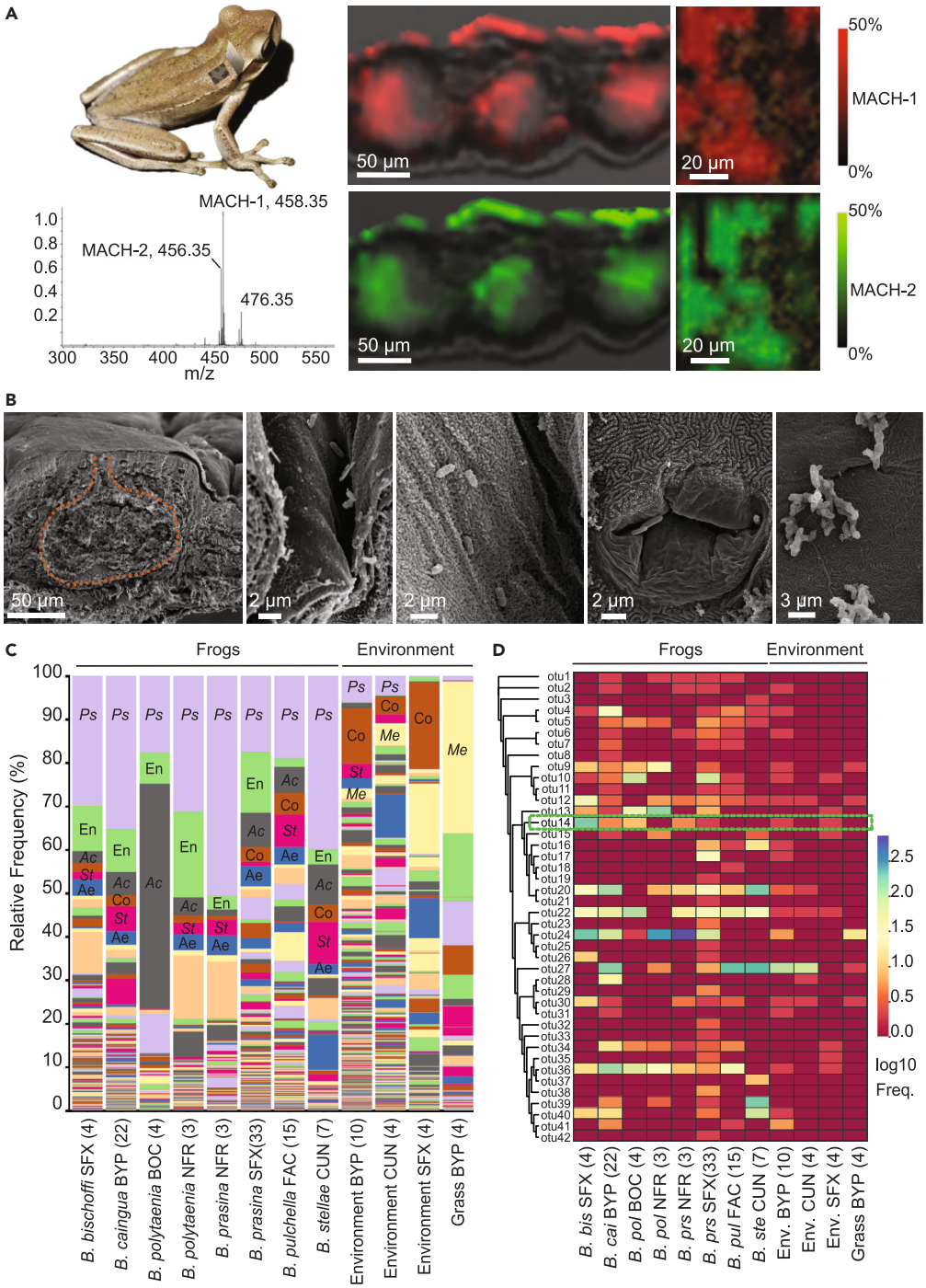

Figure 3. Macrocyclic acylcarnitines and bacteria, mainly represented by *Pseudomonas* strains, colocalize in the frog skin

(A) Ions $[M]^+$ *m/z* 456.35 (MACH-2) and $[M]^+$ *m/z* 458.35 (MACH-1) detected by *in situ* MALDI IMS in the skin of *Boana prasina* within serous glands and at the surface as observed in transverse sections (Middle graph) and the dorsal surface (Right graph).

(B) Scanning electron micrographs showing secretion granules within serous glands (dotted lines on the Left graph) in transverse sections and bacteria distribution mainly in skin folds (Middle graphs) and around pore glands (Right graphs).

(C) Mean relative abundance of bacterial OTUs present in the skin of each population and environmental samples at the genus level. *Pseudomonas* (*Ps*) is predominant in frogs' skin. Other relevant genera in frogs are *Acinetobacter* (*Ac*), *Stenotrophomonas* (*St*), and three unidentified genera of

Figure 3. *Continued*

Enterobacteriaceae (En), Comamonadaceae (Co), and Aeromonadaceae (Ae), and Methylobacterium (Me) in environmental samples. Values in parentheses indicate the number of samples for each category. Acronyms of sites are listed in Table S1.

(D) Phylogenetic tree of OTUs sequences classified as *Pseudomonas* and heatmap showing the relative abundance of these OTUs in the skin of each population and environmental samples. The green dotted rectangle depicts the sequence associated with *Pseudomonas* sp. MPFS (OTU 14), a biologically significant symbiont isolated in our previous study[14] and used in carnitine growth experiments (next section). Abbreviations, Freq., frequency.

amphibians' skin is established and maintained over time (Figure 5). In this model, while most environmental bacteria can initially reach the skin surface of tree frogs, only those with specific adaptive resistance may overcome the high concentration of host antimicrobial peptides,[17] which interacts with bacterial membranes through conserved motifs.[32] At the same time, distinct bacterial lineages, such as members of the *Pseudomonas* community capable of utilizing macrocyclic acylcarnitines as nutritional metabolites, will own significant advantages over potential microbial competitors. Once *Pseudomonas* sp. MPFS and other *Pseudomonas* have settled on the skin, they can produce antifungal metabolites like pyocyanin and sessilin that would help the host fight the pathogen *Batrachochytrium dendrobatidis*.[17] In addition, they can secrete odorous methoxypyrazines, likely mediating sexual interactions in the frog (Figure 5).[14] Thus, this model would explain the low environmental abundance of *Pseudomonas* and its prevalence on the skin of tree frogs of the *Boana pulchella* group, as well as the mutual benefits for both partners.

We then used published information from diverse families worldwide to understand whether this model can be generalized to other amphibians. Collectively, data indicate that the skin is a unique niche that can be effectively occupied by only a few bacterial taxa, despite their low relative abundance in the environment.[18–20,33] This effect is usually viewed as the consequence of host and phylogenetic factors, yet, the compounds and mechanisms involved remain poorly characterized.[18–20] In this sense, recent efforts showed that antimicrobial skin peptides function as a host's molecular filter for specific strains[17,20,34,35] and likely exert their activity to conserved motifs.[32] Given that most frogs have antimicrobial peptides and amphibians are the most common animal taxon in antimicrobial peptide databases,[36] it is reasonable to assume that skin peptides could selectively inhibit microorganisms in many amphibians' lineages. In contrast, biogenic amines[13] (i.e., low-molecular-weight nitrogenated molecules similar to carnitine) secreted by several amphibians may serve as nutritional sources to the advantage of their symbiotic partners. As shown here, such compounds would particularly benefit species of *Pseudomonas* able to use them as carbon and energy sources.[37] The significance of *Pseudomonas* in amphibians' skin has been recognized in different families because of its predominance and the production of antifungal compounds like viscosin-like peptides[38] and 2,4-diacetylphloroglucinol[16] aiding the host in fighting chytrids. In addition, members of this community were recently shown to produce tetrodotoxin[15] and methoxypyrazines,[14] suggesting an active contribution in avoiding predators and sexual interactions, respectively. Thus, our proposed model suggests that amphibians' metabolites of several lineages can actively regulate the establishment of beneficial symbionts through antimicrobial agents and nutrient provisions.

Although the skin of amphibians has been chemically examined over decades,[13] recent studies have opened up exciting research perspectives.[14,15,39] In this sense, our study represents the first characterization of a macrocyclic acylcarnitine in nature, together with a comprehensive report on the enzymes involved in the metabolism of acylcarnitines and long-chain fatty acids in amphibians' skin. Specifically, the transcriptome analysis revealed the occurrence of enzymes that in mammals are predominantly expressed in extra-dermal tissues and also the first description of these enzymes in the skin of amphibians. For example, three members of the acyl-CoA synthetase long-chain family[40] and the three isoforms of carnitine palmitoyltransferase 1, known to occur mainly in the liver (CPT1A), muscle (CPT1B), and brain (CPT1C),[26] are expressed in the skin of *B. prasina*. Likewise, we found two distinct isoforms of the superfamily of cytochrome P450 enzymes within the family 4 subfamily B member 1 (CYP4B1) to be expressed in frogs' skin, though in humans, it is predominantly expressed in lung and fat tissues.[41] Such a diverse set of enzymes linked to long-chain fatty acid metabolism supports a very active role for frogs' skin in regulating this class of compounds. In particular, the higher gene expression of CPT1 compared to CPT2 would explain the initial accumulation of acylcarnitines,[42] which would become the substrate for subsequent reactions, including ω-hydroxylation and lactonization, lastly representing an alternative mechanism to regulate excess acyl groups.

The accumulation of acylcarnitines in humans is linked to incomplete fatty acid β-oxidation, insulin resistance, and oxidative stress, reflecting a dysregulated mitochondrial metabolism.[43,44] However, the prevalence of acylcarnitines in the skin glands of frogs does not mark a metabolic disorder or a response to energetic demands. Instead, these compounds may contribute to cold acclimation, reduction of water loss, mitigation of ultraviolet A (UVA)-induced injury, and osmoprotectant as we observed these frogs to be active during freezing nights (near 0°C) and bask under direct sunlight during the day even at high altitudes. A combination of the marked amphipathic nature of acylcarnitines, the long aliphatic chain, and the charged quaternary ammonium moiety mainly supports these propositions. For example, cold acclimation in fishes is related to increased CPT1 activity and a net accretion of lipids[45] and in frogs with the accumulation of plasma carnitine.[46] Furthermore, depositing acylcarnitines on the skin surface would provide a waterproofing mechanism equivalent to the lipid mixture acting as a skin coating in other dry-adapted tree frogs.[47] Lastly, it was established that L-carnitine could mitigate UVA-induced skin injury by suppressing oxidative stress and inflammatory responses.[48] This protective role is supported by a recent study showing that 2-methylbutyrylcarnitine was upregulated in high-elevation frogs experimentally exposed to UV radiation.[49]

By characterizing amphibians' macrocyclic acylcarnitines that likely evolved as an adaptation for unique physiological roles, which also currently modulate the establishment of beneficial symbionts, our findings add a new level of complexity for surveying coevolutionary interactions. The wide distribution of carnitine in nature[25] and carnitine-catabolism pathways in *Pseudomonas* suggest they represent full-functioning mechanisms ready to be co-opted for symbiosis. Alternatively, but not mutually exclusive, the results indicate that carnitine's catabolic genes have evolved in *Pseudomonas* because of their association with many multicellular organisms.[17] Regardless of the process involved, we

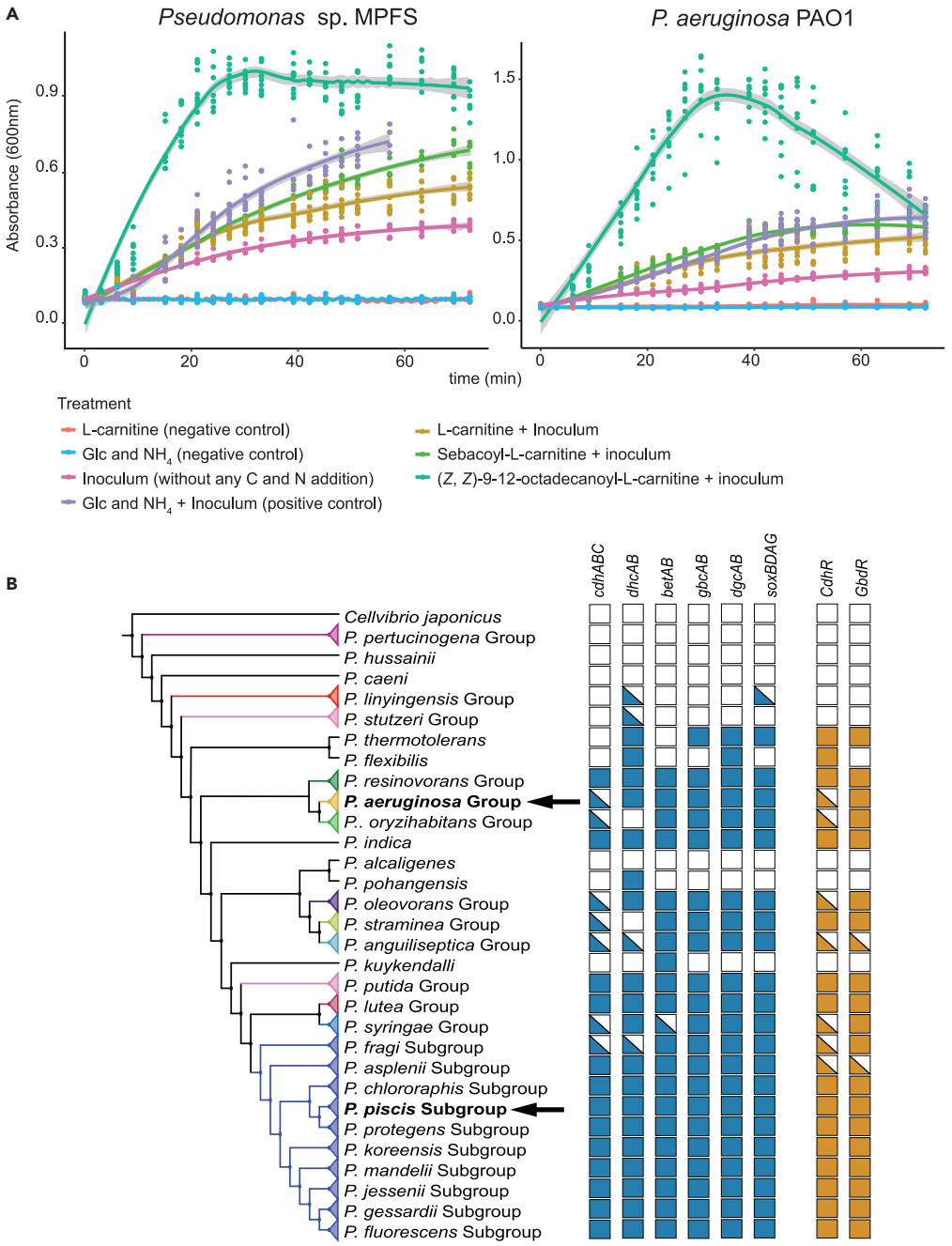

Figure 4. Carnitine and acylcarnitines serve as nutrients in *Pseudomonas*

(A) Growth curves of *Pseudomonas* sp. MPFS and *P. aeruginosa* (PAO1) show their capability to grow in media containing L-carnitine and L-acylcarnitines as the sole carbon and nitrogen source.

(B) Summary of the higher-level taxonomy of *Pseudomonas* (Left) with arrows depicting the position of the two strains used in (A). Genes involved in the catabolic pathway of carnitine (blue) or positive. Regulators (orange) of its synthetic pathway, previously described in *P. aeruginosa* (PAO1), are depicted as presence/absence in columns on the right. Filled boxes, triangles, and empty boxes show presence in all clade members, in some or none.

hypothesize that the coevolution between tree frogs and *Pseudomonas* relies on the active role of frogs' metabolites favoring the maintenance of environmental-derived microorganisms that benefit the host in short- and midterm. This idea aligns with the holobiont concept, which postulates that some symbionts can increase their population size dramatically if their metabolites improve host fitness.[3] Under this umbrella and in an analogy to the rhizosphere of plants,[8] we recommend the term "dermosphere" proposed by Assis et al.[21] to describe the skin region under the direct influence of chemicals released by the host and the associated microbiome. This term is more accurate

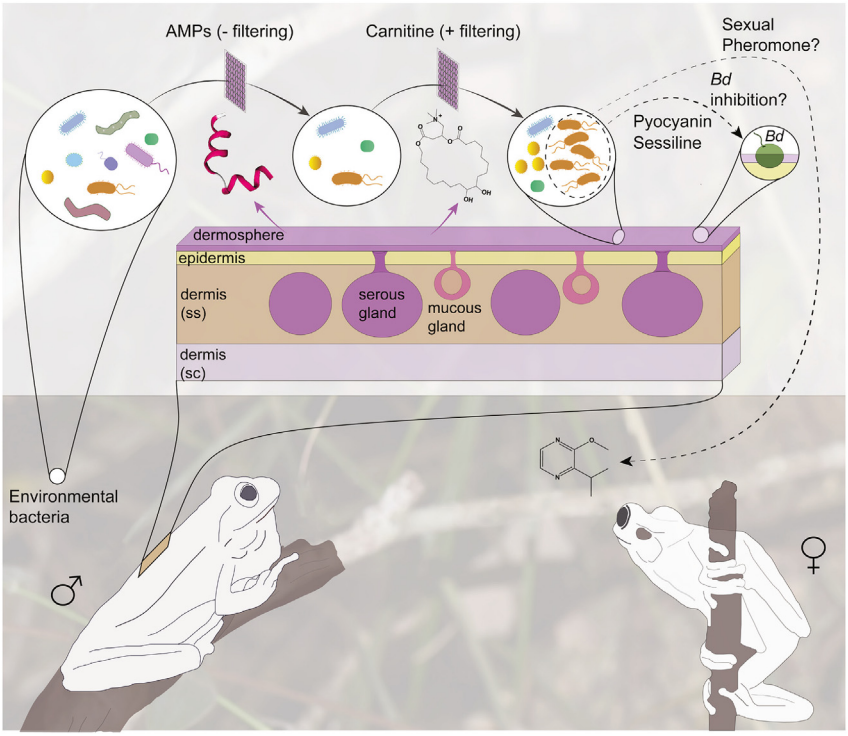

Figure 5. Simplified model for the chemical interaction between the host and Pseudomonas in the dermosphere of Boana prasina

Once on the skin, the pool of environmental bacteria may be filtered by negative (−) and positive (+) chemical factors secreted by the frog. Those that thrive in this environment may produce distinct metabolites mediating protection against pathogens and social behaviors. Abbreviations: AMPs, Antimicrobial peptides; Bd *Batrachochytrium dendrobatidis*; sc stratum compactum; ss stratum spongiosum.

than the mucosome[50] because the noun "*some*" from Ancient Greek indicates "body", denoting an enclosed compartment such as liposomes or peroxisomes, clearly not representing the open system of the skin surface. Many similarities can be recognized between the rhizosphere and the dermosphere. For instance, Hiltner proposed in his definition of rhizosphere more than 100 years ago that different plants' root exudates foster the establishment of unique bacterial communities and that the composition of these communities would influence the host's resistance to pathogens.[8] Both effects are compatible with those reported here for the host's specialized metabolites and the inhibition of the fungus *B. dendrobatidis* by various amphibians' bacterial communities described elsewhere.[51]

In conclusion, our work provides broader functional and evolutionary pictures of amphibians' metabolites while supporting an active role in shaping the skin microbiome. In our simplified model, the host secretes chemicals that indirectly, through inhibition of competitors, and positively, through nutrient provision, help the host's symbionts, which, in turn, release chemicals that positively contribute to various aspects of the host's biology. Additionally, our descriptions of lipid-related enzymes and macrocyclic acylcarnitines derivatives represent exciting research avenues for studying long-chain fatty acid metabolism in the skin and their potential link with unique physiological and protective functions in terrestrial vertebrates. This leads to the hypothesis that different host chemicals, such as acylcarnitines, primarily evolved as adaptations to other ecological roles and were subsequently co-opted to participate in symbiotic interactions. Our findings also allow for predicting a wide occurrence of similar mechanisms in the symbiosis between other vertebrate groups and their microbiomes, while the dermosphere framework may provide a more comprehensive view of the many metabolites' roles in such interactions.

Limitations of the study

Our study focused on the interaction between a specific clade of tree frogs and their skin symbionts. Although we could demonstrate that a host-specific bacterium can exploit metabolites secreted by the skin of an amphibian's species as its sole carbon and nitrogen source, our study has four major limitations. First, our study only relied on indirect evidence to extend our findings and models to other tree frogs and amphibians. Second, the biosynthetic proposal was based on enzymes identified from two transcriptomes. Third and fourth, our bacterial growth assays were conducted only on one bacterial strain as a representative of the bacterial symbiotic community of the host and using commercially available acylcarnitines rather than the macrocyclic acylcarnitines produced by the frogs. Future experiments should specifically examine MACH-1 and MACH-2, explore deeper the biosynthetic proposal, seek whether other symbionts also use amphibian skin's

metabolites as a nutritional source, investigate other metabolites that may benefit host-symbiont interaction, and include amphibians from distantly related clades.

STAR★METHODS

Detailed methods are provided in the online version of this paper and include the following:

- KEY RESOURCES TABLE
- RESOURCE AVAILABILITY
  - Lead contact
  - Materials availability
  - Data and code availability
- EXPERIMENTAL MODEL AND STUDY PARTICIPANT DETAILS
  - Frog specimens used
  - Collection permits
- METHOD DETAILS
  - Acquisition of the skin glandular secretion
  - Skin metabolic profile: HPLC-DAD ESI MS and MS/MS
  - Processing and molecular networking of mass spectrometry data
  - Isolation and purification of acylcarnitines
  - Structural elucidation of MACH-1 and MACH-2
  - Mass fragmentation patterns of MACH-1 and MACH-2
  - Optical rotatory dispersion analyses of MACH-1
  - Analysis of skin lipids
  - Skin distribution of MACH-1 and MACH-2 by MALDI-IMS imaging
  - Transcriptome annotation, quantification, and biosynthetic proposal
  - Electron microscopy analyses
  - Frogs' sampling for microbial community analyses
  - Bacterial community analysis
  - Bacterial growth assays
  - Bacterial genome analyses

SUPPLEMENTAL INFORMATION

Supplemental information can be found online at https://doi.org/10.1016/j.isci.2023.108109.

ACKNOWLEDGMENTS

We are grateful to Ricardo Silva for his many helpful suggestions while conducting this work. We also thank Pedro P. Taucce, Camila Capel Godinho, José Godinho, Luiz Fernando Carmo, Carola Jovanovich, Helio Ricardo da Silva, Javier Torres, Diego Baldo, Juan Boeris, Andrea Caballero, Miriam C. Vera, Ariadne F. Sabbag, Carla M. Lopes, Delio Baêta, Fernando Vargas Salinas, and Mauricio Rivera Correa for their help during fieldwork. Izabel Cristina Casanova Turatti, Jose Carlos Tomaz, Valquiria A. Polisel Jabor, and Felipe Calil provided valuable assistance during mass spectrometry and bacterial growth experiments and Ina Schleicher helped us during EM sample preparation. We also thank Neelu Begum and Andrew H. Moeller for their critical comments and suggestions. This project was founded by São Paulo Research Foundation FAPESP grants #2013/50954-0, #2014/50265-3, 2020/02207-5, 2021/10639-5; Coordenação de Aperfeiçoamento de Pessoal de Nível Superior (CNPq) (process #306623/2018-8); Agencia Nacional de Promoción Científica y Tecnológica grant number PICT 2020 #2939 and Consejo Nacional de Investigaciones Científicas y Técnicas (CONICET) grant #PIP 2021-2023 to (AEB); FAPESP post-doctoral fellowships #2014/20915-6 and #2017/23725-1 (AEB); #2017/17648-4 (AB); #2012/21803-1 and #2014/01651-8 (AMCR); #2017/26162-8 (MLL); #2015/01001-6 (WGPM).

AUTHOR CONTRIBUTIONS

A.E.B., M.L.L., G.M.C., J.O., and N.P.L. designed research; A.E.B., M.L.L., A.B., B.B., C.B., M.M., F.C.N., J.N.M., and W.P.M. performed research; A.E.B., M.L.L., A.B., C.B., F.C.N., W.P.M., A.M.C.R., J.O., and N.P.L. analyzed data; A.E.B., M.L.L., and M.T.P. coordinated sampling and lab work; J.O. and N.P.L. supervised microbial and chemical analyses; A.E.B., M.L.L., A.B., F.C.N., G.M.C., and J.O. wrote the paper with contributions from all authors.

DECLARATION OF INTERESTS

The authors declare no competing interests.

INCLUSION AND DIVERSITY

We support inclusive, diverse, and equitable conduct of research.

Received: May 7, 2023
Revised: July 23, 2023
Accepted: September 28, 2023
Published: October 4, 2023

REFERENCES

1. Byrd, A.L., Belkaid, Y., and Segre, J.A. (2018). The human skin microbiome. Nat. Rev. Microbiol. *16*, 143–155. https://doi.org/10.1038/nrmicro.2017.157.
2. Gilbert, S.F., Sapp, J., and Tauber, A.I. (2012). A symbiotic view of life: we have never been individuals. Q. Rev. Biol. *87*, 325–341.
3. Rosenberg, E., and Zilber-Rosenberg, I. (2016). Microbes drive evolution of animals and plants: the hologenome concept. mBio *7*, e01395.
4. McLaren, M.R., and Callahan, B.J. (2020). Pathogen resistance may be the principal evolutionary advantage provided by the microbiome. Philos. Trans. R. Soc. B *375*, 20190592.
5. Ezenwa, V.O., Gerardo, N.M., Inouye, D.W., Medina, M., and Xavier, J.B. (2012). Animal behavior and the microbiome. Science *338*, 198–199. https://doi.org/10.1126/science.1227412.
6. Chen, Y.E., Fischbach, M.A., and Belkaid, Y. (2018). Skin microbiota-host interactions. Nature *553*, 427–436. https://doi.org/10.1038/nature25177.
7. Tipton, L., Darcy, J.L., and Hynson, N.A. (2019). A developing symbiosis: enabling cross-talk between ecologists and microbiome scientists. Front. Microbiol. *10*, 292.
8. Hartmann, A., Rothballer, M., and Schmid, M. (2008). Lorenz Hiltner, a pioneer in rhizosphere microbial ecology and soil bacteriology research. Plant Soil *312*, 7–14.
9. Vieira, S., Sikorski, J., Dietz, S., Herz, K., Schrumpf, M., Bruelheide, H., Scheel, D., Friedrich, M.W., and Overmann, J. (2020). Drivers of the composition of active rhizosphere bacterial communities in temperate grasslands. ISME J. *14*, 463–475.
10. Adair, K.L., and Douglas, A.E. (2017). Making a microbiome: the many determinants of host-associated microbial community composition. Curr. Opin. Microbiol. *35*, 23–29.
11. Mergaert, P. (2018). Role of antimicrobial peptides in controlling symbiotic bacterial populations. Nat. Prod. Rep. *35*, 336–356. https://doi.org/10.1039/c7np00056a.
12. Bosch, T.C.G. (2013). Cnidarian-microbe interactions and the origin of innate immunity in metazoans. Annu. Rev. Microbiol. *67*, 499–518. https://doi.org/10.1146/annurev-micro-092412-155626.
13. Erspamer, V. (1994). Bioactive secretions of the amphibian integument. In Amphibian biology. Volume 1: The integument, H. Heatwole and G. Barthalmus, eds. (Surrey Beatty & Sons), pp. 178–350.
14. Brunetti, A.E., Lyra, M.L., Melo, W.G.P., Andrade, L.E., Palacios-Rodríguez, P., Prado, B.M., Haddad, C.F.B., Pupo, M.T., and Lopes, N.P. (2019). Symbiotic skin bacteria as a source for sex-specific scents in frogs. Proc. Natl. Acad. Sci. USA *116*, 2124–2129.
15. Vaelli, P.M., Theis, K.R., Williams, J.E., O'Connell, L.A., Foster, J.A., and Eisthen, H.L. (2020). The skin microbiome facilitates adaptive tetrodotoxin production in poisonous newts. Elife *9*, e53898.
16. Woodhams, D.C., LaBumbard, B.C., Barnhart, K.L., Becker, M.H., Bletz, M.C., Escobar, L.A., Flechas, S.V., Forman, M.E., Iannetta, A.A., Joyce, M.D., et al. (2018). Prodigiosin, violacein, and volatile organic compounds produced by widespread cutaneous bacteria of amphibians can inhibit two *Batrachochytrium* fungal pathogens. Microb. Ecol. *75*, 1049–1062.
17. Brunetti, A.E., Bunk, B., Lyra, M.L., Fuzo, C.A., Marani, M.M., Spröer, C., Haddad, C.F.B., Lopes, N.P., and Overmann, J. (2022). Molecular basis of a bacterial-amphibian symbiosis revealed by comparative genomics, modeling, and functional testing. ISME J. *16*, 788–800.
18. Walke, J.B., Becker, M.H., Loftus, S.C., House, L.L., Cormier, G., Jensen, R.V., and Belden, L.K. (2014). Amphibian skin may select for rare environmental microbes. ISME J. *8*, 2207–2217. https://doi.org/10.1038/ismej.2014.77.
19. McKenzie, V.J., Bowers, R.M., Fierer, N., Knight, R., and Lauber, C.L. (2012). Co-habiting amphibian species harbor unique skin bacterial communities in wild populations. ISME J. *6*, 588–596.
20. Flechas, S.V., Acosta-González, A., Escobar, L.A., Kueneman, J.G., Sánchez-Quitian, Z.A., Parra-Giraldo, C.M., Rollins-Smith, L.A., Reinert, L.K., Vredenburg, V.T., Amézquita, A., and Woodhams, D.C. (2019). Microbiota and skin defense peptides may facilitate coexistence of two sympatric Andean frog species with a lethal pathogen. ISME J. *13*, 361–373.
21. Assis, A.B.d., Barreto, C.C., and Navas, C.A. (2017). Skin microbiota in frogs from the Brazilian Atlantic Forest: Species, forest type, and potential against pathogens. PLoS One *12*, e0179628. https://doi.org/10.1371/journal.pone.0179628.
22. Faivovich, J., et al. (2021). Phylogenetic relationships of the *Boana pulchella* group (Anura: Hylidae). Mol. Phylogenetics Evol. *155*, 106981.
23. Rebouche, C.J., and Paulson, D.J. (1986). Carnitine metabolism and function in humans. Annu. Rev. Nutr. *6*, 41–66.
24. Ramsay, R.R., and Zammit, V.A. (2004). Carnitine acyltransferases and their influence on CoA pools in health and disease. Mol. Aspects Med. *25*, 475–493.
25. Bremer, J. (1983). Carnitine–metabolism and functions. Physiol. Rev. *63*, 1420–1480.
26. Bonnefont, J.-P., Djouadi, F., Prip-Buus, C., Gobin, S., Munnich, A., and Bastin, J. (2004). Carnitine palmitoyltransferases 1 and 2: biochemical, molecular and medical aspects. Mol. Aspects Med. *25*, 495–520.
27. Lopes-Marques, M., Delgado, I.L.S., Ruivo, R., Torres, Y., Sainath, S.B., Rocha, E., Cunha, I., Santos, M.M., and Castro, L.F.C. (2015). The origin and diversity of Cpt1 genes in vertebrate species. PLoS One *10*, e0138447.
28. Meadows, J.A., and Wargo, M.J. (2015). Carnitine in bacterial physiology and metabolism. Microbiology *161*, 1161–1174.
29. Meadows, J.A., and Wargo, M.J. (2018). Transcriptional regulation of Carnitine catabolism in *Pseudomonas aeruginosa* by CdhR. mSphere *3*, e00480-17.
30. Kleber, H.-P. (1997). Bacterial carnitine metabolism. FEMS Microbiol. Lett. *147*, 1–9.
31. Wargo, M.J., and Hogan, D.A. (2009). Identification of genes required for *Pseudomonas aeruginosa* carnitine catabolism. Microbiology *155*, 2411–2419.
32. Brunetti, A.E., Fuzo, C.A., Aguilar, S., Rivera-Correa, M., Marani, M.M., and Lopes, N.P. (2023). The significance of hypervariability and conserved motifs in antimicrobial peptides from tree frogs. J. Nat. Prod. *86*, 1761–1769.
33. Ellison, S., Rovito, S., Parra-Olea, G., Vásquez-Almazán, C., Flechas, S.V., Bi, K., and Vredenburg, V.T. (2019). The influence of habitat and phylogeny on the skin microbiome of amphibians in Guatemala and Mexico. Microb. Ecol. *78*, 257–267.
34. Loudon, A.H., Kurtz, A., Esposito, E., Umile, T.P., Minbiole, K.P.C., Parfrey, L.W., and Sheafor, B.A. (2020). Columbia spotted frogs (*Rana luteiventris*) have characteristic skin microbiota that may be shaped by cutaneous skin peptides and the environment. FEMS Microbiol. Ecol. *96*, fiaa168.
35. Woodhams, D.C., Rollins-Smith, L.A., Reinert, L.K., Lam, B.A., Harris, R.N., Briggs, C.J., Vredenburg, V.T., Patel, B.T., Caprioli, R.M., Chaurand, P., et al. (2020). Probiotics modulate a novel amphibian skin defense peptide that is antifungal and facilitates growth of antifungal bacteria. Microb. Ecol. *79*, 192–202.
36. Lazzaro, B.P., Zasloff, M., and Rolff, J. (2020). Antimicrobial peptides: Application informed by evolution. Science *368*, eaau5480.
37. Luengo, J.M., and Olivera, E.R. (2020). Catabolism of biogenic amines in *Pseudomonas* species. Environ. Microbiol. *22*, 1174–1192.
38. Christian Martin, H., Ibáñez, R., Nothias, L.-F., Boya P, C.A., Reinert, L.K., Rollins-Smith, L.A., Dorrestein, P.C., and Gutiérrez, M. (2019). Viscosin-like lipopeptides from frog skin bacteria inhibit *Aspergillus fumigatus* and *Batrachochytrium dendrobatidis* detected by imaging mass spectrometry and molecular networking. Sci. Rep. *9*, 1–11.
39. Taboada, C., Brunetti, A.E., Lyra, M.L., Fitak, R.R., Faigón Soverna, A., Ron, S.R., Lagorio, M.G., Haddad, C.F.B., Lopes, N.P., Johnsen, S., et al. (2020). Multiple origins of green

coloration in frogs mediated by a novel biliverdin-binding serpin. Proc. Natl. Acad. Sci. USA *117*, 18574–18581.
40. Mashek, D.G., Li, L.O., and Coleman, R.A. (2006). Rat long-chain acyl-CoA synthetase mRNA, protein, and activity vary in tissue distribution and in response to diet. J. Lipid Res. *47*, 2004–2010.
41. Jarrar, Y.B., and Lee, S.-J. (2019). Molecular functionality of cytochrome P450 4 (CYP4) genetic polymorphisms and their clinical implications. Int. J. Mol. Sci. *20*, 4274.
42. Thumelin, S., Esser, V., Charvy, D., Kolodziej, M., Zammit, V.A., McGarry, D., Girard, J., and Pegorier, J.P. (1994). Expression of liver carnitine palmitoyltransferase I and II genes during development in the rat. Biochem. J. *300*, 583–587.
43. Dambrova, M., Makrecka-Kuka, M., Kuka, J., Vilskersts, R., Nordberg, D., Attwood, M.M., Smesny, S., Sen, Z.D., Guo, A.C., Oler, E., et al. (2022). Acylcarnitines: Nomenclature, biomarkers, therapeutic potential, drug targets, and clinical trials. Pharmacol. Rev. *74*, 506–551.
44. Aguer, C., McCoin, C.S., Knotts, T.A., Thrush, A.B., Ono-Moore, K., McPherson, R., Dent, R., Hwang, D.H., Adams, S.H., and Harper, M.E. (2015). Acylcarnitines: potential implications for skeletal muscle insulin resistance. FASEB J *29*, 336–345.
45. Rodnick, K.J., and Sidell, B.D. (1994). Cold acclimation increases carnitine palmitoyltransferase I activity in oxidative muscle of striped bass. Am. J. Physiol. *266*, R405–R412.
46. Voituron, Y., Eugene, M., and Barré, H. (2003). Survival and metabolic responses to freezing by the water frog (*Rana ridibunda*). J. Exp. Zool. Comp. Exp. Biol. *299*, 118–126.
47. Lillywhite, H.B. (2006). Water relations of tetrapod integument. J. Exp. Biol. *209*, 202–226.
48. Salama, S.A., Arab, H.H., Omar, H.A., Gad, H.S., Abd-Allah, G.M., Maghrabi, I.A., and Al Robaian, M.M. (2018). L-carnitine mitigates UVA-induced skin tissue injury in rats through downregulation of oxidative stress, p38/c-Fos signaling, and the proinflammatory cytokines. Chem. Biol. Interact. *285*, 40–47.
49. Fu, T.-T., Sun, Y.-B., Gao, W., Long, C.-B., Yang, C.-H., Yang, X.-W., Zhang, Y., Lan, X.-Q., Huang, S., Jin, J.-Q., et al. (2022). The highest-elevation frog provides insights into mechanisms and evolution of defenses against high UV radiation. Proc. Natl. Acad. Sci. USA *119*. e2212406119.
50. Woodhams, D.C., Brandt, H., Baumgartner, S., Kielgast, J., Küpfer, E., Tobler, U., Davis, L.R., Schmidt, B.R., Bel, C., Hodel, S., et al. (2014). Interacting symbionts and immunity in the amphibian skin mucosome predict disease risk and probiotic effectiveness. PLoS One *9*, e96375. https://doi.org/10.1371/journal.pone.0096375.
51. Becker, M.H., Walke, J.B., Murrill, L., Woodhams, D.C., Reinert, L.K., Rollins-Smith, L.A., Burzynski, E.A., Umile, T.P., Minbiole, K.P.C., and Belden, L.K. (2015). Phylogenetic distribution of symbiotic bacteria from Panamanian amphibians that inhibit growth of the lethal fungal pathogen *Batrachochytrium dendrobatidis*. Mol. Ecol. *24*, 1628–1641.
52. Huerta-Cepas, J., Szklarczyk, D., Heller, D., Hernández-Plaza, A., Forslund, S.K., Cook, H., Mende, D.R., Letunic, I., Rattei, T., Jensen, L.J., et al. (2019). eggNOG 5.0: a hierarchical, functionally and phylogenetically annotated orthology resource based on 5090 organisms and 2502 viruses. Nucleic Acids Res. *47*, D309–D314.
53. Bray, N.L., Pimentel, H., Melsted, P., and Pachter, L. (2016). Near-optimal probabilistic RNA-seq quantification. Nat. Biotechnol. *34*, 525–527.
54. Lechner, M., Findeiß, S., Steiner, L., Marz, M., Stadler, P.F., and Prohaska, S.J. (2011). Proteinortho: detection of (co-)orthologs in large-scale analysis. BMC Bioinf. *12*, 124. https://doi.org/10.1186/1471-2105-12-124.
55. Brunetti, A.E., Hermida, G.N., Iurman, M.G., and Faivovich, J. (2016). Odorous secretions in anurans: Morphological and functional assessment of serous glands as a source of volatile compounds in the skin of the treefrog *Hypsiboas pulchellus* (Amphibia: Anura: Hylidae). J. Anat. *228*, 430–442. https://doi.org/10.1111/joa.12413.
56. Wang, M., Carver, J.J., Phelan, V.V., Sanchez, L.M., Garg, N., Peng, Y., Nguyen, D.D., Watrous, J., Kapono, C.A., Luzzatto-Knaan, T., et al. (2016). Sharing and community curation of mass spectrometry data with Global Natural Products Social Molecular Networking. Nat. Biotechnol. *34*, 828–837. https://doi.org/10.1038/nbt.3597.
57. Kessner, D., Chambers, M., Burke, R., Agus, D., and Mallick, P. (2008). ProteoWizard: open source software for rapid proteomics tools development. Bioinformatics *24*, 2534–2536.
58. Pluskal, T., Castillo, S., Villar-Briones, A., and Orešič, M. (2010). MZmine 2: modular framework for processing, visualizing, and analyzing mass spectrometry-based molecular profile data. BMC Bioinf. *11*, 395.
59. Myers, O.D., Sumner, S.J., Li, S., Barnes, S., and Du, X. (2017). Detailed investigation and comparison of the XCMS and MZmine 2 chromatogram construction and chromatographic peak detection methods for preprocessing mass spectrometry metabolomics data. Anal. Chem. *89*, 8689–8695.
60. Shannon, P., Markiel, A., Ozier, O., Baliga, N.S., Wang, J.T., Ramage, D., Amin, N., Schwikowski, B., and Ideker, T. (2003). Cytoscape: a software environment for integrated models of biomolecular interaction networks. Genome Res. *13*, 2498–2504.
61. Bligh, E.G., and Dyer, W.J. (1959). A rapid method of total lipid extraction and purification. Can. J. Biochem. Physiol. *37*, 911–917.
62. Kozich, J.J., Westcott, S.L., Baxter, N.T., Highlander, S.K., and Schloss, P.D. (2013). Development of a dual-index sequencing strategy and curation pipeline for analyzing amplicon sequence data on the MiSeq Illumina sequencing platform. Appl. Environ. Microbiol. *79*, 5112–5120.
63. Bolyen, E., Rideout, J.R., Dillon, M.R., Bokulich, N.A., Abnet, C.C., Al-Ghalith, G.A., Alexander, H., Alm, E.J., Arumugam, M., Asnicar, F., et al. (2019). Reproducible, interactive, scalable and extensible microbiome data science using QIIME 2. Nat. Biotechnol. *37*, 852–857.
64. Amir, A., McDonald, D., Navas-Molina, J.A., Kopylova, E., Morton, J.T., Zech Xu, Z., Kightley, E.P., Thompson, L.R., Hyde, E.R., Gonzalez, A., and Knight, R. (2017). Deblur rapidly resolves single-nucleotide community sequence patterns. mSystems *2*, e00191-16.
65. Price, M.N., Dehal, P.S., and Arkin, A.P. (2010). FastTree 2–approximately maximum-likelihood trees for large alignments. PLoS One *5*, e9490.
66. Miller, J.H. (1972). Experiments in Molecular Genetics (Cold Spring Harbor Laboratory Press).
67. Stover, C.K., Pham, X.Q., Erwin, A.L., Mizoguchi, S.D., Warrener, P., Hickey, M.J., Brinkman, F.S., Hufnagle, W.O., Kowalik, D.J., Lagrou, M., et al. (2000). Complete genome sequence of *Pseudomonas aeruginosa* PAO1, an opportunistic pathogen. Nature *406*, 959–964. https://doi.org/10.1038/35023079.
68. Bastard, K., Smith, A.A.T., Vergne-Vaxelaire, C., Perret, A., Zaparucha, A., De Melo-Minardi, R., Mariage, A., Boutard, M., Debard, A., Lechaplais, C., et al. (2014). Revealing the hidden functional diversity of an enzyme family. Nat. Chem. Biol. *10*, 42–49.
69. Bazire, P., Perchat, N., Darii, E., Lechaplais, C., Salanoubat, M., and Perret, A. (2019). Characterization of L-carnitine metabolism in *Sinorhizobium meliloti*. J. Bacteriol. *201*, e00772-18.

STAR★METHODS

KEY RESOURCES TABLE

REAGENT or RESOURCE	SOURCE	IDENTIFIER
Bacterial and virus strains		
Pseudomonas sp. MPFS	Brunetti et al.[14,17]	N/A
Pseudomonas aeruginosa PAO1	DSMZ (German Collection of Microorganisms and Cell Cultures)	DSM 22644
Biological samples		
Details of frog specimens is listed in Table S1	This study	N/A
Chemicals, peptides, and recombinant proteins		
Ultra-pure water	Mili-Q, Millipore	N/A
Acetonitrile	J.T. Baker	ID No JT-9012-03
TFA-Na^+	Sigma-Aldrich	ID No 132101
Methanol d_4 (99.8% purity)	Sigma-Aldrich	ID No 151947
α-cyano-4-hydroxycinnamic acid matrix	Bruker	ID No 248-879-1
Glucose	Sigma-Aldrich	ID No 1181302
$ClNH_4$	Sigma-Aldrich	ID No 213330
L-carnitine	Sigma-Aldrich	ID No 8.40092
sebacoyl-L-carnitine	Sigma-Aldrich	ID No 16329
(*Z*,*Z*)-9-12-octadecanoyl-L-carnitine	Sigma-Aldrich	ID No 76771
Critical commercial assays		
DNeasy blood and tissue extraction kit	Qiagen	ID No 69506
Deposited data		
GNPS metabolic data	This paper	MassIVE MSV0000924999
Skin microbial community data	This paper	NCBI-SRA PRJNA Acc. No. 498895
Pseudomonas sp. MPFS complete genome	Brunetti et al.[17]	NCBI-Genbank Acc. No. NZ_CP066123.1
Pseudomonas spp. OTU sequences	This paper	NCBI-Genbank Acc. No. OR335663–OR335704
Raw transcriptome data	Brunetti et al.[17]	NCBI-SRA PRJNA Acc. No. 675859
Accession numbers for *Pseudomonas* spp. genomes	See Data S2	See Data S2
Experimental models: Organisms/strains		
Pseudomonas sp. MPFS	Brunetti et al.[14,17]	N/A
Pseudomonas aeruginosa PAO1	DSMZ (German Collection of Microorganisms and Cell Cultures)	DSM 22644
Oligonucleotides		
Barcode primers of the V4 region of the bacterial 16S rRNA gene	https://earthmicrobiome.org/protocols-and-standards/16s/	515F (Parada) and 806R (Apprill)
Software and algorithms		
DataAnalysis 4.0	Bruker	https://www.bruker.com/protected/en/services/software-downloads/mass-spectrometry/software-solutions.html
MSConvert	MSConvert	https://proteowizard.sourceforge.io/index.html
MZmine2-2.53	MZmine	http://mzmine.github.io/

(*Continued on next page*)

Continued

REAGENT or RESOURCE	SOURCE	IDENTIFIER
GNPS platform	GNPS	https://gnps.ucsd.edu/ProteoSAFe/static/gnps-splash.jsp
Cytoscape 3.8.0	Cytoscape	https://cytoscape.org/index.html
TopSpin 3.5	Bruker	https://www.bruker.com/en/products-and-solutions/mr/nmr-software/topspin.html
GCMS Solution	Shimadzu	https://www.shimadzu.com/an/products/gas-chromatograph-mass-spectrometry/gc-ms-software/gcmssolution/index.html
FlexImaging v.2.1	Bruker	https://www.bruker.com/protected/en/services/software-downloads/mass-spectrometry/software-solutions.html
ITEM Software	ITEM Software	https://cfim.ku.dk/equipment/electron_microscopy/cm100/iTEM_Main_Brochure.pdf
QIIME2 v2020.11	Qiime2	https://qiime2.org/
R-4.2.3	R Core Team	https://www.R-project.org/
eggnog-mapper v2	Huerta-Cepas et al.[52]	http://eggnog-mapper.embl.de/
Kallisto	Bray et al.[53]	https://github.com/pachterlab/kallisto
ProteinOrtho v4.26	Lechner et al.[54]	https://gitlab.com/paulklemm_PHD/proteinortho/

RESOURCE AVAILABILITY

Lead contact

- Further information and requests for resources should be directed to and will be fulfilled by the lead contact, Andrés E. Brunetti (aebrunetti@conicet.gov.ar, andresbrunetti@gmail.com).

Materials availability

- This study did not generate new unique reagents.

Data and code availability

- Metabolomic data generated in this study are deposited at MassIVE: MSV0000924999
- The sequences of the bacterial amplicon libraries and *Pseudomonas* spp. OTU sequences were deposited at NCBI-SRA PRJNA: 498895 and NCBI-GenBank: OR335663–OR335704, respectively.
- The skin transcriptome of *Boana prasina* and the complete genome of *Pseudomonas* sp. MPFS, were available at NCBI-SRA PRJNA: 675859 and NCBI-GenBank: NZ_CP066123.1, respectively.
- This study did not generate original codes. All data were analyzed following the protocols and instructions from the software, packages, and workflows available in the original publications or repositories.
- Any additional information required to reanalyze the data reported in this paper is available from the lead contact upon request.

EXPERIMENTAL MODEL AND STUDY PARTICIPANT DETAILS

Frog specimens used

Twenty-one adult specimens of the South American treefrog *Boana prasina* were collected at two sites in São Paulo and Rio de Janeiro, Brazil (Table S1). In addition, adult specimens from 33 species representing 11 genera of the tree frog subfamilies Hylinae and Phyllomedusinae were collected in different localities from Brazil, Colombia, and Argentina (Table S1). Because of our particular interest in species related to *B. prasina*, specific efforts were made to collect representatives from the *B. pulchella* group, resulting in the collection of eight species (*B. bischoffi*, *B. caingua*, *B. curupi*, *B. polyteania*, *B. prasina*, *B. pulchella*, *B. riojana*, and *B. stellae*). These species represent four of the five recognized clades within this group. For all species, we included male and female specimens. Detailed information on species identity, location, and coordinates are listed in Table S1. In all cases, individuals were transported to the laboratory and kept in glass terraria at 22°C–26°C with a 12 h photoperiod, provided with dechlorinated tap water, access to refugia, and fed with small crickets. They were housed in these conditions for 2 to 4 days before sampling. After sampling, they were euthanized with a lethal dose of lidocaine 20% applied in the pelvic region. Vouchers are housed at "Célio F. B. Haddad Amphibians collections" at The State University of São Paulo, Rio Claro, Sao Paulo,

Brazil; at the Museo de Herpetología Universidad de Antioquia (MHUA) in Medellín, Colombia; and at the Herpetological Collection of the Laboratorio de Genética Evolutiva, Instituto de Biología Subtropical (Unam-CONICET), Posadas, Misiones, Argentina.

Collection permits

All procedures involving frogs were carried out according to the regulations specified by Conselho Nacional de Controle de Experimentação Animal (CONCEA), Ministério da Ciência, Tecnologia e Inovação (MCTI) and were approved by the Ethics Committee on Animal Use (CEUA) of School of Pharmaceutical Sciences of Ribeirão Preto- (17.1.1074.60.0), Brazil. Collection permits were issued by Instituto Chico Mendes de Conservação da Biodiversidade (ICMBio) / SISBIO, Brasil (Permits 41508-8, 50071-1, 50071-2, 57098-1), Autoridad Nacional de Licencias Ambientales (ANLA), Colombia (Permits 1177-Oct 9th 2014 to the Universidad de Los Andes and 0524 May 27th 2014 to the Universidad de Antioquia), and Ministerio de Ecología y Recursos Naturales Renovables de Misiones (035/2017) and Instituto Misioneiro de Biodiversidad (IMiBio), Argentina (Permits 11/2021).

METHOD DETAILS

Acquisition of the skin glandular secretion

The skin glandular secretion of each frog was sampled from the dorsal skin region using the following protocol: the skin was cleaned and moistened with ultrapure water obtained from an Ultra Centrifugal Filter Unit (Milli-Q, Millipore). Subsequently, an electrical stimulus (1–2 V, pulse length 2–4 ms) was applied during 8–10 s using two platinum electrodes rubbed gently along the animal's dorsum.[55] Finally, the secretion was washed off with 20–30 mL of the sterilized water collected in falcon tubes (50 mL), frozen in liquid N_2, lyophilized, and stored refrigerated at -20°C.

Skin metabolic profile: HPLC-DAD ESI MS and MS/MS

Analyses of liquid chromatography hyphenated to diode array detection and electrospray ionization tandem mass spectrometry (LC-DAD-MS/MS) were performed in an ultra-fast liquid chromatography (UFLC) instrument (Shimadzu, Japan). The UFLC instrument was coupled to a high-resolution mass spectrometer micrOTOF-QII (Bruker Daltonics, Billerica – USA). The dried glandular secretion was dissolved in water: acetonitrile (7:3) with 0.1% (v/v) trifluoroacetic acid (TFA) at a final concentration of 0.5 mg mL^{-1} and centrifuged. The supernatant was injected into a C_{18} - Luna Kinetex Phenomonex® (100 mm x 2.1 mm x 2.6 μm) column, with the temperature adjusted to 35°C. The mobile phase (flow 0.25 mL/min) consisted of water (A) and acetonitrile (B) in the following gradient: 0.0–35.0 min (15–80% B); 35.0–37.0 min (80–100% B); 37.0–42.0 min (100% B); 42.0–45.0 min (100–15% B); 45.0–48.0 min (15% B). qTOF acquisition parameters were as follows: capillary 3.5 kV, end plate offset 500 V, nebulizer 35 psi, dry gas (N_2) with a flow of 8.0 L/min, and temperature of 300°C. Accurate masses were obtained using TFA-Na^+ (sodiated trifluoroacetic acid) as the internal standard. Mass spectra were measured between *m/z* 90 to1200 in the positive ion mode. ESI-MS/MS fragments were generated by collision-induced dissociation using nitrogen as the collision gas (5–50 eV depending on the *m/z* of each precursor ion) and analyzed with the autoMSn mode using the Enhanced Resolution Mode for MS and UltraScan.

Processing and molecular networking of mass spectrometry data

Molecular networking[56] workflows organize large data sets of tandem mass spectra based on the similarity between fragmentation patterns of different but related precursor ions. The LC-QTOF-MS/MS raw data were converted to mzXML format using the MSConvert software[57] for molecular networking. First, isotope grouping, alignment, and data normalization were processed with MZmine2-2.53[58] with the following parameters: an MS1 noise level of 1.0E10^{3} ^{and}; an MS2 noise level of 1.0E10^{2}. Next, chromatograms were built with the ADAP chromatogram builder module with the following parameters: min highest intensity, 1.5E10^{3}; maximum *m/z* tolerance, 10 ppm. Next, they were deconvoluted using the ADAP (Wavelets) module[59] with the following parameters: S/N threshold, 10; min feature height, 10; coefficient/area threshold, 110; peak duration range, 0.01–2.0 min; retention time wavelet range, 0.001–0.1 s. Next, the fragmentation spectra were paired to the deconvoluted peaks using 0.01 Da and 0.3 min windows, and the LC-MS features (isotopologues, adducts, and in-source fragments) were annotated using the peak grouping module with the following parameters: deisotope, true; *m/z* tolerance, ten ppm; retention time tolerance, 2 min; maximum charge, 3. Finally, the features were aligned with the Join Aligner module using the following parameters: tolerance, 5 ppm; weight for *m/z*, 75.0; retention time tolerance, 0.2 min; weight for retention time, 25.0.

The feature table and spectral data were exported and uploaded to the GNPS platform[56] and analyzed with the feature-based molecular network workflow. Molecular features in the form of MS/MS spectra were putatively identified against matches to the MS2-based public spectral library based on the cosine score similarity (above 0.7) and setting six as the minimum number of shared peaks. The parameters and results will be available at the MassIVE repository from the GNPS platform.[56] The results were subsequently visualized in Cytoscape 3.8.0.[60] The molecular networking file contained the scan number, precursor *m/z*, and fragment *m/z* ions were colored at different taxonomic levels [species within the *Boana pulchella* group (i.e., *B. pulchella* clade, *B. riojana* clade, *B. semiguttata* clade, and *B. polytaenia* clade), group for other species within the genus *Boana*, genus for other species of Cophomantini, and subfamily in the remaining species].

Isolation and purification of acylcarnitines

The dried skin glandular secretion of ten individuals of *Boana prasina* was pooled (50 mg), resuspended in water (TFA 0.01%): methanol (4:6), and centrifuged. Afterward, the supernatant was fractionated by a chromatographic column containing Sephadex as the stationary phase

(LH-20) using water (TFA 0.01%): and methanol (3:7) as the mobile phase. The purified fractions containing cyclic acylcarnitines were pooled, and the compounds were isolated using a C18 - Luna (Phenomonex® – 250 mm × 21.2 mm x 5 μm) preparative column equilibrated with 70% water (TFA 0.01%) (eluent A) and 30% methanol (eluent B). The elution profile was a gradient produced by a CBM-20A System controlling two LC-20AP HPLC pumps (Shimadzu, MD, USA) at a flow rate of 21 mL/min as follows: 0.0–45.0 min (30–70% B); 45.0–50.0 min (70−100% B); 50.0–55.0 min (100% B); 55.0–60.0 min (100−30% B); 60.0–65.0 (30% B). Eluents were monitored by UV absorbance at 220 nm. Fractions were collected using an automated fraction collector FRC-10A (Shimadzu, USA), concentrated, and vacuum-dried for subsequent analysis. Two main ions corresponding to MACH-1 ($C_{25}H_{48}NO_6$; *m/z* 458) and MACH-2 ($C_{25}H_{46}NO_6$; *m/z* 456) were detected by direct infusion into the ESI source by the syringe pump and analyzed by an ultrOTOF Q-II (Bruker Daltonics, Billerica – USA) mass spectrometer. The isolated cyclic acylcarnitines MACH-1 and MACH-2 were obtained as viscous, transparent oil yielding 0.6 mg (12%) and 0.4 mg (8%), respectively. They were next submitted to liquid chromatography-tandem mass spectrometry (LC-DAD-MS/MS) to assess their purity. The samples were lyophilized and stored at −20°C for further experiments (NMR, mass spectrometry, optical rotatory dispersion, and derivatization). Both purified compounds are colorless viscous oils.

Structural elucidation of MACH-1 and MACH-2

The purified samples of the cyclic acylcarnitines were dried under nitrogen gas, dissolved in methanol-d_4 99.8% (Sigma-Aldrich), transferred to 3 mm micro-NMR tubes, and analyzed. The ^{1}H NMR spectra were recorded at 25°C on a 14.1 Tesla Bruker Avance III spectrometer operating at a proton NMR frequency of 600.13 MHz (Bruker, Karlsruhe, Germany). Chemical shifts are given in δ units (ppm) relative to tetramethylsilane. All analyses were performed using TopSpin 3.5 (Bruker).

Several NMR experiments were performed for both cyclic acylcarnitines. Free induction decays (FIDs) were Fourier transformed, and the spectra were manually phased and baseline corrected. ^{1}H -^{1}H COSY experiments were performed using a spectral window of -0.33−9.88 ppm. ^{1}H-^{13}C direct coupling was studied by HMQC, using a spectral window of -0.33−9.88 ppm for the F2 dimension (^{1}H) and -15−220 ppm for the F1 dimension (^{13}C). Finally, ^{1}H-^{13}C HMBC data were obtained using a spectral width of -0.33−9.88 ppm for the F2 dimension (^{1}H) and -20–210 ppm for the F1 dimension (^{13}C).

Because of NMR's limitations in assigning the positions of the two hydroxyl groups in the fatty acid chain, we derivatized and then analyzed the acylcarnitine *m/z* 458 with a Shimadzu (Kyoto, Japan) GC coupled to a Mass Spectrometer Detector (GC/MS QP2010 Plus). We first conducted mild alkaline hydrolysis for the derivatization process, for which the sample was dissolved in H_2O: EtOH: KOH 2M (10:10:2) and heated at 40°C for 1 h. Next, it was acidified with HCl to a final pH = 5, and the free acids were extracted into ethyl acetate: diethyl ether (1:1) and derivatized (20 μl, BSTFA, 80°C, 1 h). The derivatized sample was then injected in the GC/MS (2 μl) equipped with a Restek Rtx® -5MS column (60 m×0.25 mm×0.25 μm) obtained from Restek (Bellefonte, PA, USA) using helium (purity of 99.9999%; White Martins, RS, Brazil) with a flow rate of 1.4 mL/min as the carrier gas. The oven temperature was programmed as follows: initial temperature of 70°C (5 min hold), 8°C/min to 330°C (60 min hold). The injector was operated in split mode (1:5) at a temperature of 280°C. A quadrupole mass spectrum detector was operated in electron impact mode at 70 eV and 250°C with a mass range of 35–700 u. The GC/MS spectra were analyzed using the GCMS Solution software.

High-resolution mass spectrometry analysis and 1D [^{13}C (only for MACH01) and ^{1}H] and 2D NMR experiments (HMBC, HMQC, and COSY) enable the unequivocal assignment of all the atoms in the 4-trimethylazaniumyl-butanoate moiety. In addition, these data allowed us to determine that the aliphatic region of MACH-1 and MACH-2 correspond to dehydroxylated C18 fatty acids likely derived from oleate and linoleate, respectively. Furthermore, NMR data allow determining that the two hydroxyl groups were in adjacent carbons because there were only two Carbon atoms with δ = 33 ppm. If, for instance, there were one or two carbon atoms between the two carbons bearing the -OH, we would expect two or four carbons, with NMR signals around δ 45 ppm and δ 33 ppm, respectively, which was not observed in the experiments. Finally, the precise location of the hydroxyls in the aliphatic chain was determined after fatty acid hydrolysis, followed by silylation and GCMS analysis, which allowed us to assign them to C9′ and C10′ unambiguously.

Mass fragmentation patterns of MACH-1 and MACH-2

Purified fractions containing the cyclic acylcarnitines *m/z* 456 and *m/z* 458 from *Boana prasina* were submitted to high-resolution MS/MS analysis and MS/MS and MS^3 analyses in the Ion Trap mass spectrometer AmaZon (Bruker Daltonics, Billerica – USA). Samples were introduced into the ESI source by a syringe pump and analyzed by a micrOTOFQ (Bruker Daltonics, Billerica – USA) mass spectrometer. Accurate mass analyses were performed using a solution of sodium trifluoroacetic acid [(TFA)n+Na]$^+$ as the internal standard. The parameters were as follows: capillary voltage 3.5 kV, end plate offset of 500 V, the capillary temperature at 200°C; nitrogen as the sheath gas; drying gas flow at 4.0 L/min; drying gas temperature at 180°C; nebulizer gas pressure of 0.4 bar; positive ESI mode. Mass spectra were measured from *m/z* 50–600 in the positive ion mode. Fragmentation patterns of cyclic acylcarnitine were proposed considering the high-resolution MS/MS for molecular formulae determination (accurate molecular weights < 5ppm) and ions generated in the MS^3 experiments (submitted as MassIVE dataset). Retention time (shift tolerance of ±0.05 min) was used as orthogonal information on peak annotation.

Optical rotatory dispersion analyses of MACH-1

The optical rotatory dispersion of the acylcarnitine MACH-1 was measured using a Jasco P2000 spectropolarimeter (Nikota, Japan) to determine whether the molecule is dextro- or levorotatory. After NMR analyses, the methanol-d_4 was evaporated, and the sample was resuspended in methanol. Measures were taken at 25°C in triplicate using a 1 mL cuvette.

Analysis of skin lipids

After euthanasia, the dorsal skin of adult specimens of *Boana prasina* and *B. bischoffi* was removed, macerated under liquid nitrogen, and transferred to a 5 mL glass vial. The lipids were extracted using the protocol described by Bligh & Dyer (1959)[61] as a guide. A 3.75 mL mixture of chloroform: methanol (2:1) was added to the macerated skin and submitted to ultrasound for 10 min and vortex for 2 min. Then, 1.25 mL of Mili-Q water was added to the homogenate and submitted to a second row of ultrasound and vortex. The homogenate was filtered through a Whatman 1 filter paper on a Buchner funnel with slight suction, the content was transferred to a test tube, left at room temperature for a few minutes, and centrifuged (3 min, 1000 rpm). The volume of the chloroform layer containing the lipid fraction was gently removed with a glass pipet, transferred to a 5 mL glass tube, evaporated to dryness under gaseous N_2, and stored at 20°C.

The lipid fraction was dissolved in chloroform and separated in a thin-layer chromatography plate (silica gel 60 F_{254}) using hexane: ethyl ether: acetic acid (80: 30: 2) as the mobile phase. Lipids were detected by iodine staining. Individual components were scraped from the plates and submitted to derivatization with alkylation reagents. Lipid derivatization was performed by dissolving the dry sample in 500 μL of BF_3 in methanol, vortexed for 1 min, and maintaining it at 80°C for 10 min. Afterward, samples were immediately cooled on ice, followed by the addition of 500 μL of Mili-Q water and 1 mL of pentane, and then vortexed for 1 min. Next, the homogenate was centrifuged (3 min, 3000 rpm), the pentane phase containing the ester derivatives was collected gently, transferred to a 1.5 mL tube, evaporated to dryness under gaseous N_2, and stored at -20°C.

The derivatized lipids were dissolved with 50–100 μL of hexane. Next, 2 μL were injected in the GC/MS Shimadzu QP2010 Plus (Kyoto, Japan) equipped with a ZB-Wax column (30 m × 0.25 mm×0.25 μm) obtained from Restek (Bellefonte, PA, USA). Helium (purity of 99.9999%; White Martins, RS, Brazil) with a 1.3 mL/min flow rate was used as the carrier gas. The oven temperature was programmed as follows: initial temperature of 50°C (3 min hold), 10°C/min to 200°C (5min hold), 5°C/min to a final temperature of 240°C (20 min hold). The injector was operated in splitless mode (1.5 min sampling time) at a temperature of 230°C. A quadrupole mass spectrum detector was operated in electron impact mode at 70 eV and 250°C with a mass range of 40–500 u. The spectra were analyzed using the GCMS Solution software.

Skin distribution of MACH-1 and MACH-2 by MALDI-IMS imaging

For observations of skin on transverse sections, dorsal skin samples from two male specimens of *Boana prasina* were removed, immediately embedded in carboxymethyl cellulose 2%, and frozen at -20°C. Then, the samples were sliced at 10 μm in a cryotome (CM1860 Cryostat, Leica Biosystem, Nussloch, Germany) at -20°C. Both transverse and whole skin sections were first mounted on indium tin oxide-coated glass slides for MALDI imaging (Bruker Daltonic, Bremen, Germany). Next, they were coated with Imageprep (Bruker Daltonic, Bremen, Germany) using sixty cycles with a solution of 7 mg mL−1 of an α-cyano-4-hydroxycinnamic acid matrix in 50% acetonitrile/water with 0.2% TFA. Each cycle was based on spraying, filling the chamber with nitrogen, and drying.

MALDI-Imaging analyses were performed using a MALDI-TOF/TOF (Bruker Daltonics, UltrafleXtreme, Bremen, Germany) system equipped with a smart beam-II laser system controlled by a FleXcontrol v.3.3 (Bruker Daltonics, Bremen, Germany), employing AutoXecute mode. IMS data were analyzed and normalized using FlexImaging v.2.1 (Bruker Daltonics). The settings of the instrument were as follows: positive ion reflector mode; ion source 1, 25.00 kV; ion source 2, 22.35 kV; lens, 7.75 kV; reflector, 26.60 kV; reflector 2, 13.30 kV; pulsed ion extraction, 100 ns; laser frequency, 100 Hz; and matrix suppression mass cutoff, *m/z* 500. The spectra were recorded across a mass range of *m/z* 100−600, accumulating 500 shots per spectrum. The images were collected from transverse sections and skin surface at a 20 μm spatial resolution in both x and y directions using MS positive ion mode. Quercetin and skin extracts of *B. prasina* were used as the external calibration of the mass spectrometer and to validate the detection of MACH-1 and MACH-2 by MALDI, respectively. The average mass deviation was below 10 ppm. MS/MS analysis directly from the skin was performed to confirm assignments of the two mains cyclic acylcarnitines in positive-ion reflector mode using LIFT fragmentation.

Transcriptome annotation, quantification, and biosynthetic proposal

The reference transcriptome assembled from one male and one female specimen in Brunetti et al.[17] was annotated using the eggnog-mapper v2 available online[52] with the following parameters: seed ortholog e-value 0.001, seed ortholog score 60, and query cover 20. The level of expressions of different genes was estimated from the cleaned reads of the male and the female using Kallisto.[53] Based on the molecule structure, the annotation, and published information, we searched for enzymes associated with carnitine biosynthesis, the formation of the acylcarnitine ester ω-oxidation of fatty acids, epoxidation, and hydroxylation. The similarity of these proteins was compared with those annotated in humans and *Xenopus laevis* and retrieved from Uniprot. Transcriptome annotation and quantification were performed to determine whether the skin of *Boana prasina* possesses the enzymes for the biosynthesis of the cyclic acylcarnitines, to assess the relevance of these enzymes, and to propose a biosynthesis pathway for these compounds.

Electron microscopy analyses

Dorsal skin samples of *Boana prasina* were fixed with various concentrations of formaldehyde and glutaraldehyde and stored in a fixative solution upon electronic microscopy sample preparation. The skin was divided into fragments to perform scanning electron microscopy (SEM) and transmission electron microscopy (TEM).

For SEM, the skin was washed twice with TE buffer to remove the fixative. Dehydration was performed in a graded series of acetone (10, 30, 50, 70, and 90%) on ice, each step for 10 minutes, followed by two 10 minutes steps with 100% acetone at room temperature. Afterward, critical-point drying with liquid CO_2 (CPD 30, Balzers, Liechtenstein) was done. The skin fragments were placed with conductive tapes on aluminum stubs and covered with a palladium–gold film by sputter coating (SCD 500, Bal-Tec, Liechtenstein). The skin was examined from two views, surface and transverse sections. Visualization was conducted with a field emission scanning electron microscope (Merlin, Zeiss, Germany) using the HESE2 Everhart Thornley SE detector, the in-lens SE detector, and an acceleration voltage of 5 kV.

For TEM, the fixed samples were washed for 40 minutes with 0.1 M EM-HEPES buffer (HEPES 0.1 M, 0.09 M sucrose, 10 mM CaCl2, 10 mM MgCl2, pH 6.9) and exposed to osmium tetroxide (1% in HEPES buffer) for 1 h at room temperature. After another washing step with HEPES buffer, samples were dehydrated with a graded series (10, 30, 50, 70, 90, and 2x 100%) of acetone, each step for 30 minutes on ice, respectively, at room temperature (100 % steps). In the 70% EtOH step, we added 2% uranyl acetate (UAc) and incubated overnight at 4°C. Samples were subsequently infiltrated with the low viscosity (LV) resin (1:1, 2:1, 2 × 100%), each step incubating for a minimum of 8 h. Samples were polymerized at 75°C for 15 h followed by a second polymerization step to mount the rotated flat-embedded sample block onto a resin pedestal to allow vertical sections of the skin. Ultrathin sections of approx. 50–70 nm was prepared with an Ultramicrotome (Reichelt Jung / Leica Microsystems, Germany) collected onto butvar-coated 300 mesh grids and counterstained with 4% aqueous uranyl acetate for 3 min and lead citrate for 15 seconds. Images were acquired with a transmission electron microscope TEM 910 and a Libra 120 Plus (both Zeiss, Germany) with an acceleration voltage of 80 kV and 120 kV, respectively, and at calibrated magnifications. Contrast and brightness were adjusted using the ITEM software.

Frogs' sampling for microbial community analyses

Forty-five adult *B. prasina* specimens were collected at the margins of a small lake at São Francisco Xavier, São Paulo, Brazil (Table S1). Forty were released at the same collecting site after swabbing, and the remaining were kept as vouchers. In addition, adult specimens from five other species (*B. bischoffi*, *B. caingua*, *B. polytaenia*, *B. pulchella*, and *B. stellae*) of the *B. pulchella* group were collected at different sites in Brazil and Argentina. Each frog was handled with new gloves minimizing cross-contamination. Before swabbing, each specimen was rinsed with sterilized deionized water to eliminate transient bacteria. The dorsal skin was swabbed for all specimens within 12 h after collection using sterile MW113 swabs (Medical Wire & Equipment, Corsham, UK). In addition, environmental samples were collected by swabbing the water and grass at three sites. After sampling, each swab was immediately placed in sterile microcentrifuge vials and frozen in a -20°C freezer. Detailed information on the species, specimen numbers, location, coordinates, and voucher numbers for the frogs used in this section are listed in Table S1. Collection permits were issued by SISGEN (A1FC113, A9EC80A, A299B7D).

Bacterial community analysis

Genomic DNA was extracted from skin swabs and environmental and sterile water controls using the DNeasy blood and tissue extraction kit (Qiagen). The V4 region of the bacterial 16S rRNA gene was PCR-amplified using a dual-index approach with barcoded primers 515F and 806R.[62] PCR reactions were performed in duplicates. Negative controls for the DNA extraction and PCR mix were included to check for contamination. PCR products of each sample were pooled, purified using a DNA Gel Extraction Kit (Norgen Biotek Corp, Torold, ON, Canada), and sequenced with paired-end 2x250 v2 chemistry on an Illumina MiSeq sequencer at TUCF genomics (Boston, MA, USA). The sequences of the amplicon libraries were deposited in the NCBI short read database (SI Appendix, Data S2 A, and BioProject ID obtained after submission).

The sequences were processed and analyzed in QIIME2 v2020.11[63] on Ubuntu 20.4 LTS Linux. Briefly, the sequences were demultiplexed, paired-ends were merged, quality filtered, and denoised using Deblur workflow.[64] The Operational Taxonomic Units (OTUs) in negative controls and less than one frog sample were filtered out. The remaining sequences were aligned, and the FastTree2[65] was used to build a phylogenetic tree of OTUs using QIIME 2 standard procedures. OTUs were classified using the q2-feature-classifier-sklearn against the Greengenes 13.8 database, with 99% similarity with the OTUs reference sequences (from the 515F/806R region of the sequences). Samples were rarefied to 1,500 reads. Descriptive analyses were conducted to assess bacterial richness and similarities between frog populations and the environment.

Because we were interested in the symbiosis between frogs from the *Boana pulchella* group and bacterial strains from the *Pseudomonas* genus, we extracted from the analysis those OTU sequences classified within this genus. These sequences were compared with the sequences reported in our previous work on the bacterial community analyses from different populations of *B. prasina* obtained from culture-dependent and culture-independent methods. In addition, a heatmap was constructed within Qiime2 to depict the relative abundance variation of those OTUs identified as *Pseudomonas* spp. in all samples.

Bacterial growth assays

Pseudomonas sp. MPFS isolated from the dorsal skin of *Boana prasina* and *P. aeruginosa* PAO1 were grown for 72 h at 30°C in Mueller-Hinton (MH) broth medium and inoculated at a final absorbance at 600 nm of ~0.05 into M9 minimal medium supplemented with a specific carbon and nitrogen source.

Assays were conducted in 1 mL on 96-well polystyrene plates. For experiments, L-carnitine and two acylcarnitines (i.e., sebacoyl-L-carnitine and (*Z,Z*)-9-12-octadecanoyl-L-carnitine) purchased from Sigma-Aldrich were added to the M9 minimal medium[66] at a final concentration of 20 mM without the addition of any other carbon and nitrogen source. Positive growth controls contained glucose and NH_4Cl in the M9 medium. In contrast, negative controls either received the inoculum but lacked nitrogen and carbon sources or were supplemented with nitrogen

and carbon sources but lacked the inoculum. Plates were incubated at 30°C, and OD600 was determined every 3 or 6 h for 72 h using a microplate spectrophotometer (Infinite M200 Pro, Tecan AG, Mannedorf, Switzerland). All tests were performed in triplicate according to the Clinical and Laboratory Standards Institute (2012). Growth curves were constructed for each treatment based on their data distribution using the locally weighted regression loess curves in R. A standard procedure was used to determine differences between treatments. Briefly, the maximum growth rate and 95% confidence interval were calculated from the log-linear part of growth curves from each AMP concentration and the control treatment without AMPs. When the confidence intervals for an AMP treatment and control did not overlap, they were judged to be significantly different.

Bacterial genome analyses

Since the description of its genome in 2000,[67] *Pseudomonas aeruginosa* PAO1 has been the subject of many gene functional analyses, which yielded significant insights into the enzymes involved in the different metabolic processes of this bacterium. This information served as a reference for genomic analyses of host-symbiont systems in vertebrates, mainly because most studies have focused on *P. aeruginosa* as a human pathogen. Genes related to the catabolism of acylcarnitine as the sole source of carbon and nitrogen were obtained from published studies.[29,31,68,69]

Genes involved in the catabolism of acylcarnitines were identified in the genus *Pseudomonas* using the same data matrix from our previous work.[17] This matrix was based on 159 strains, from which 141 corresponded to type strains (Data S2). In addition, gene orthology was assessed using ProteinOrtho v4.26,[53] and the phylogenetic distribution of genes involved in the acylcarnitine catabolism was evaluated using the same phylogenetic hypothesis described previously.[17]